

Confronting the Challenge of Modeling Cloud and Precipitation Microphysics

Hugh Morrison¹ , Marcus van Lier-Walqui² , Ann M. Fridlind³ ,
Wojciech W. Grabowski¹ , Jerry Y. Harrington⁴, Corinna Hoose⁵ , Alexei Korolev⁶ ,
Matthew R. Kumjian⁴ , Jason A. Milbrandt⁷, Hanna Pawlowska⁸ , Derek J. Posselt⁹,
Olivier P. Prat¹⁰, Karly J. Reimel⁴, Shin-Ichiro Shima¹¹ , Bastiaan van Dierenhoven² ,
and Lulin Xue¹ 

Key Points:

- Microphysics is an important component of weather and climate models, but its representation in current models is highly uncertain

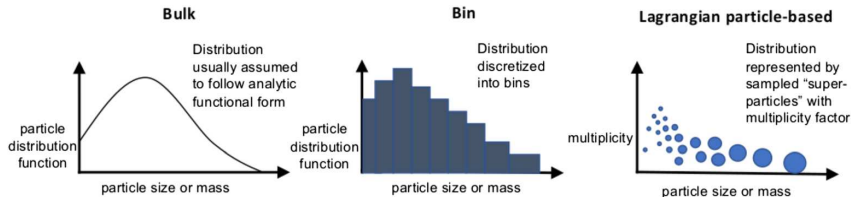


Figure 3. Representation of cloud and precipitation particle distributions in the three main types of microphysics

COMMISSIONED
MANUSCRIPT

10.1029/2019MS001689

Confronting the Challenge of Modeling Cloud and Precipitation Microphysics

Hugh Morrison¹ , Marcus van Lier-Walqui² , Ann M. Fridlind³ ,
Wojciech W. Grabowski¹ , Jerry Y. Harrington⁴, Corinna Hoose⁵ , Alexei Korolev⁶ ,
Matthew R. Kumjian⁴ , Jason A. Milbrandt⁷, Hanna Pawlowska⁸ , Derek J. Posselt⁹,
Olivier P. Prat¹⁰, Karly J. Reimel⁴, Shin-Ichiro Shima¹¹ , Bastiaan van Dierenhoven² ,
and Lulin Xue¹ 

Key Points:

- Microphysics is an important component of weather and climate models, but its representation in current models is highly uncertain

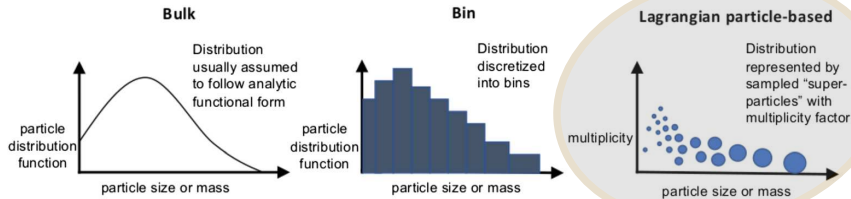
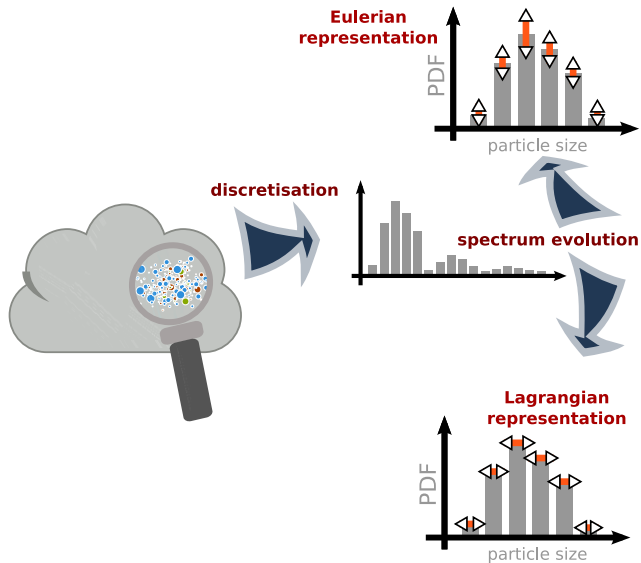
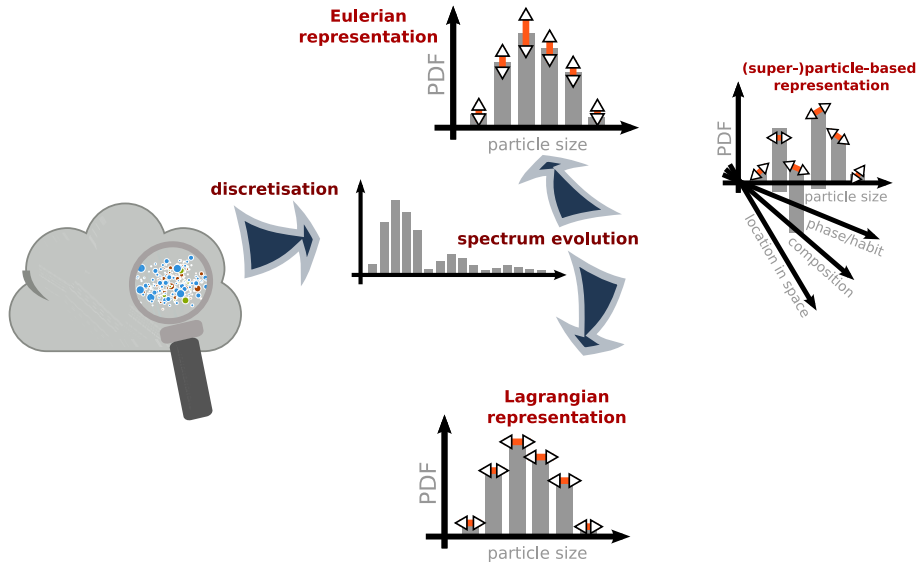


Figure 3. Representation of cloud and precipitation particle distributions in the three main types of microphysics

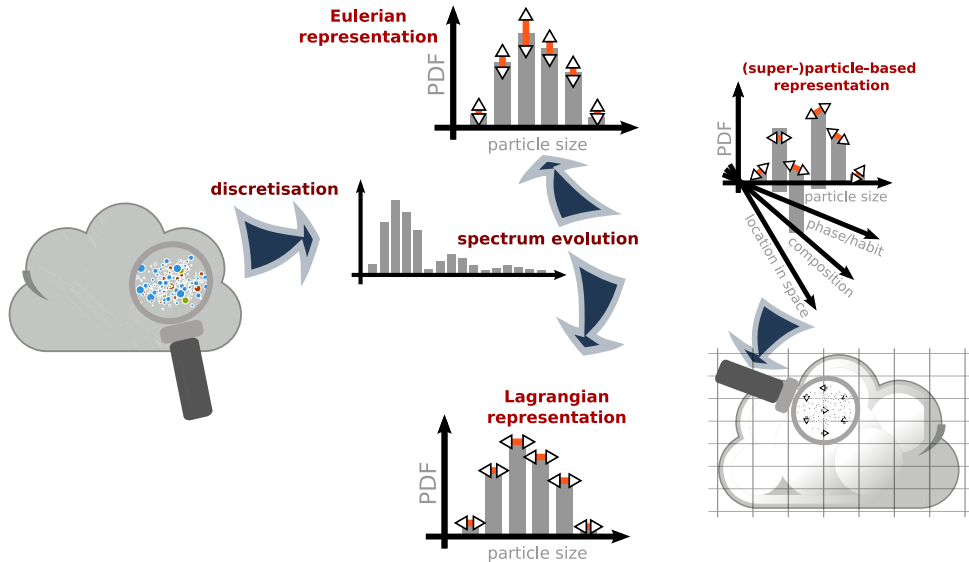
modelling cloud μ -physics: Eulerian vs. Lagrangian approaches



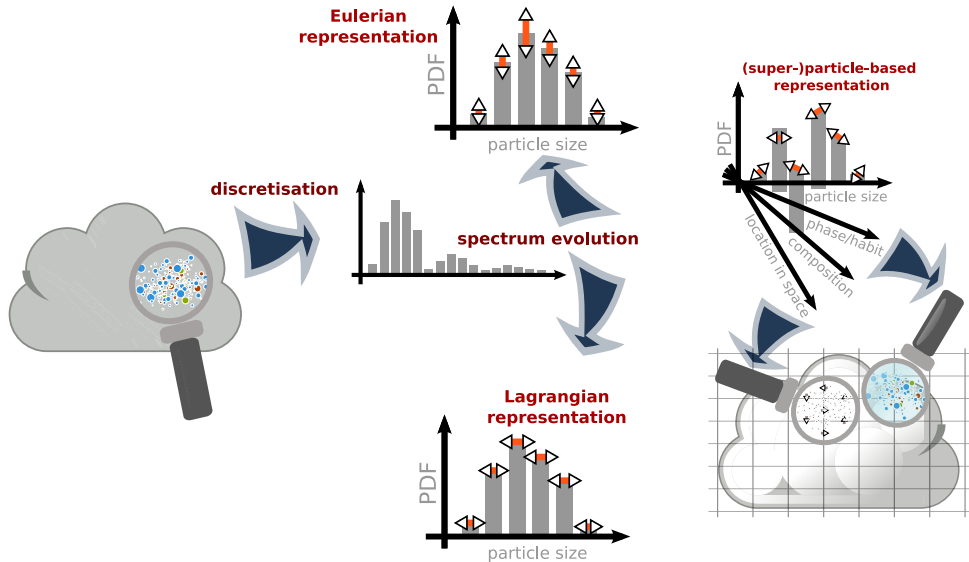
modelling cloud μ -physics: Eulerian vs. Lagrangian approaches



modelling cloud μ -physics: Eulerian vs. Lagrangian approaches



modelling cloud μ -physics: Eulerian vs. Lagrangian approaches



Lagrangian approaches: moving-sectional, particle-based, probabilistic

^aHowell 1949 (J. Atmos. Sci.): "The growth of cloud drops in uniformly cooled air"

^bLange 1978 (J. Appl. Meteorol.): "ADPIC – A Three-Dimensional Particle-in-Cell Model for the Dispersal of Atmospheric Pollutants ..."

^cZannetti 1983 (Appl. Math. Model.): "New Monte Carlo scheme for simulating Lagrangian particle diffusion with wind shear effects"

^dJacobson 2005 (Cambridge Univ. Press): "Fundamentals of Atmospheric Modelling"

^eShima et al. 2009 (QJRM): "The super-droplet method for the numerical simulation of clouds and precipitation"

Lagrangian approaches: moving-sectional, particle-based, probabilistic

- ▶ **Howell 1949^a**: "*... drop-size spectrum ... cannot be integrated analytically ... experience enables the computer to select the proper independent variables ... seven classes of nuclei ... a group of uniform drops*"

^aHowell 1949 (J. Atmos. Sci.): "The growth of cloud drops in uniformly cooled air"

^bLange 1978 (J. Appl. Meteorol.): "ADPIC – A Three-Dimensional Particle-in-Cell Model for the Dispersal of Atmospheric Pollutants ..."

^cZannetti 1983 (Appl. Math. Model.): "New Monte Carlo scheme for simulating Lagrangian particle diffusion with wind shear effects"

^dJacobson 2005 (Cambridge Univ. Press): "Fundamentals of Atmospheric Modelling"

^eShima et al. 2009 (QJRM): "The super-droplet method for the numerical simulation of clouds and precipitation"

Lagrangian approaches: moving-sectional, particle-based, probabilistic

- ▶ **Howell 1949^a**: " ... *drop-size spectrum ... cannot be integrated analytically ... experience enables the computer to select the proper independent variables ... seven classes of nuclei ... a group of uniform drops*"
- ▶ **Lange 1978^b**: " *Eulerian-Lagrangian particle-in-cell method... numerical diffusion is eliminated ... each marker particle can be tagged with its coordinates, age since generation, mass, activity, species and size ... relatively fast running in part because computations are only made for those cells that contain particles*"
- ▶ **Zannetti 1983^c**: " *Monte Carlo techniques ... output represents just one realization ... 'superparticles', i.e. simulation particles representing a cloud of physical particles having similar characteristics ... air pollution*"
- ▶ **Jacobson 2005^d**: "section 13.5 Evolution of size distributions over time
 - ▶ *full-moving structure is analogous to Lagrangian horizontal advection*
 - ▶ *core particle material is preserved during growth*
 - ▶ *eliminates numerical diffusion during growth*
 - ▶ *problems during nucleation, coagulation ... not used in three-dimensional models*"
- ▶ **Shima et al. 2009^e**: " *„super-droplet is a kind of coarse-grained view of droplets both in real space and attribute space ...cost ... becomes lower than the spectral (bin) method when the number of attributes becomes larger than ... 2~4*"
- ▶ concomitantly, related developments in aerosol and oceanic research, astrophysics, industrial simulations

^aHowell 1949 (J. Atmos. Sci.): "The growth of cloud drops in uniformly cooled air"

^bLange 1978 (J. Appl. Meteorol.): "ADPIC – A Three-Dimensional Particle-in-Cell Model for the Dispersal of Atmospheric Pollutants ..."

^cZannetti 1983 (Appl. Math. Model.): "New Monte Carlo scheme for simulating Lagrangian particle diffusion with wind shear effects"

^dJacobson 2005 (Cambridge Univ. Press): "Fundamentals of Atmospheric Modelling"

^eShima et al. 2009 (QJRMMS): "The super-droplet method for the numerical simulation of clouds and precipitation"

Shima, Sato, Hashimoto & Misumi 2020 (GMD):

Predicting the morphology of ice particles in deep convection using the super-droplet method

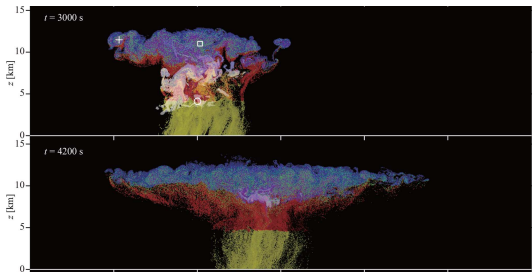


Figure 1. Typical realization of CTRL cloud spatial structures at $t = 2040, 2460, 3000, 4200,$ and 5400 s. The mixing ratio of cloud water, rainwater, cloud ice, graupel, and snow aggregates are plotted in fading white, yellow, blue, red, and green, respectively. The symbols indicate examples of unrealistic predicted ice particles (Sects. 7.3 and 9.1). See also Movie 1 in the video supplement.

Shima, Sato, Hashimoto & Misumi 2020 (GMD):

Predicting the morphology of ice particles in deep convection using the super-droplet method

- ▶ Eulerian component: momentum, heat, moisture budget
- ▶ Lagrangian component: super particles representing aerosol, water droplets, ice particles (porous spheroids)

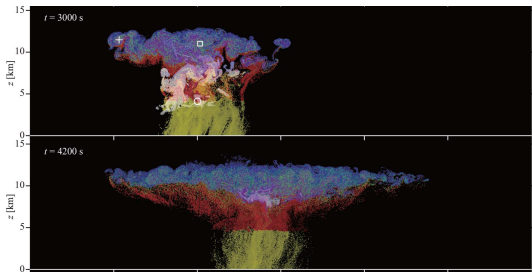


Figure 1. Typical realization of CTRL cloud spatial structures at $t = 2040, 2460, 3000, 4200,$ and 5400 s. The mixing ratio of cloud water, rainwater, cloud ice, graupel, and snow aggregates are plotted in fading white, yellow, blue, red, and green, respectively. The symbols indicate examples of unrealistic predicted ice particles (Sects. 7.3 and 9.1). See also Movie 1 in the video supplement.

Shima, Sato, Hashimoto & Misumi 2020 (GMD):

Predicting the morphology of ice particles in deep convection using the super-droplet method

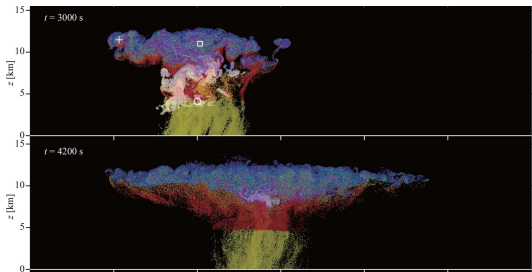
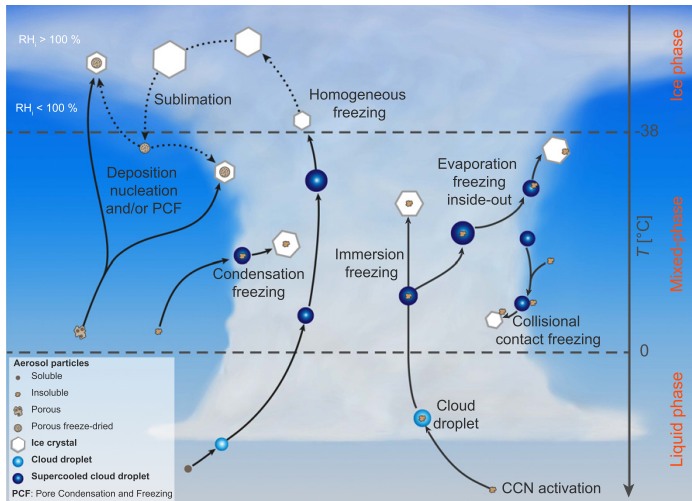


Figure 1. Typical realization of CTRL cloud spatial structures at $t = 2040, 2460, 3000, 4200,$ and 5400 s. The mixing ratio of cloud water, rainwater, cloud ice, graupel, and snow aggregates are plotted in fading white, yellow, blue, red, and green, respectively. The symbols indicate examples of unrealistic predicted ice particles (Sects. 7.3 and 9.1). See also Movie 1 in the video supplement.

- ▶ Eulerian component: momentum, heat, moisture budget
- ▶ Lagrangian component: super particles representing aerosol, water droplets, ice particles (porous spheroids)
- ▶ particle-resolved processes:
 - advection and sedimentation
 - homogeneous and immersion freezing (singular)
 - melting
 - condensation and evaporation (incl. CCN [de]activation)
 - deposition and sublimation
 - collisions (coalescence, riming, aggregation, washout)

immersion freezing and other ice crystal formation pathways in clouds



Kanji et al. 2017, graphics F. Mahrt, <https://doi.org/10.1175/AMSMONOGRAPHS-D-16-0006.1>

Journal of Geophysical Research: Atmospheres

RESEARCH ARTICLE

10.1002/2016JD025251

Key Points:

- Very ice active Snomax protein aggregates are fragile and their ice nucleation ability decreases over months of freezer storage
- Partitioning of ice active protein aggregates into the immersion oil reduces the droplet's measured freezing temperature
- Caution is warranted in the use of

The unstable ice nucleation properties of Snomax[®] bacterial particles

Michael Polen¹, Emily Lawlis¹, and Ryan C. Sullivan¹

¹Center for Atmospheric Particle Studies, Carnegie Mellon University, Pittsburgh, Pennsylvania, USA

Abstract Snomax[®] is often used as a surrogate for biological ice nucleating particles (INPs) and has recently been proposed as an INP standard for evaluating ice nucleation methods. We have found the immersion freezing properties of Snomax particles to be substantially unstable, observing a loss of ice nucleation ability

Journal of Geophysical Research: Atmospheres

RESEARCH ARTICLE

10.1002/2016JD025251

Key Points:

- Very ice active Snomax protein aggregates are fragile and their ice nucleation ability decreases over months of freezer storage
- Partitioning of ice active protein aggregates into the immersion oil reduces the droplet's measured freezing temperature
- Caution is warranted in the use of

The unstable ice nucleation properties of Snomax® bacterial particles

Michael Polen¹, Emily Lawlis¹, and Ryan C. Sullivan¹

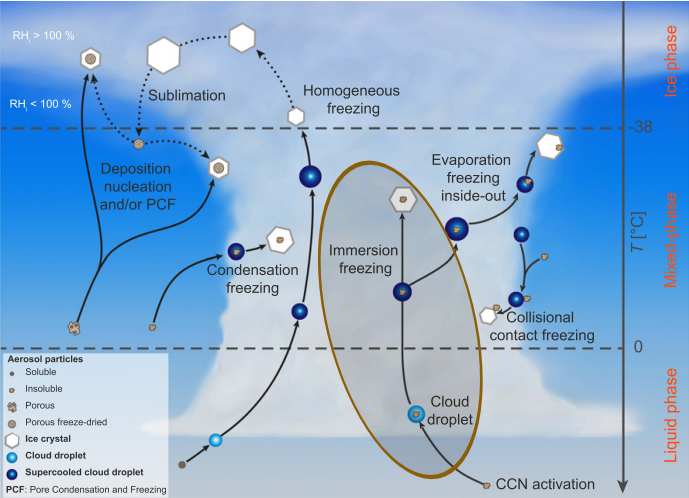
¹Center for Atmospheric Particle Studies, Carnegie Mellon University, Pittsburgh, Pennsylvania, USA

Abstract Snomax® is often used as a surrogate for biological ice nucleating particles (INPs) and has recently been proposed as an INP standard for evaluating ice nucleation methods. We have found the immersion freezing properties of Snomax particles to be substantially unstable, observing a loss of ice nucleation ability



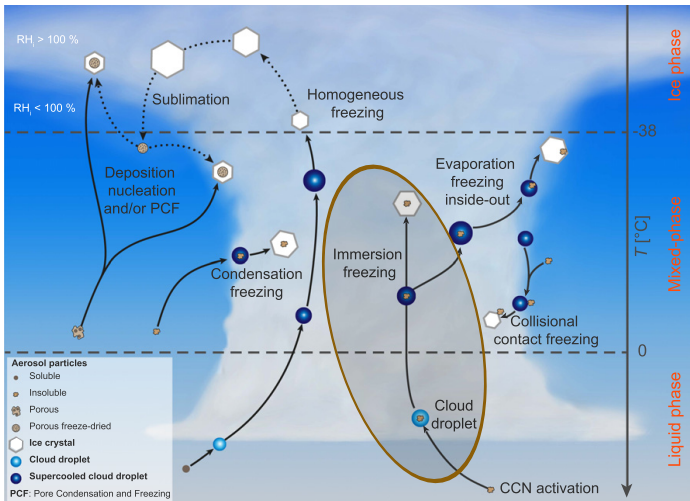
<https://www.reuters.com/markets/commodities/making-snow-stick-wind-challenges-winter-games-slope-makers-2021-11-29/>

immersion freezing and other ice crystal formation pathways in clouds

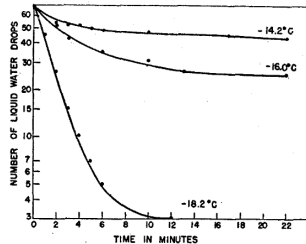


Kanji et al. 2017, graphics F. Mahrt, <https://doi.org/10.1175/AMSMONOGRAPHS-D-16-0006.1>

immersion freezing and other ice crystal formation pathways in clouds



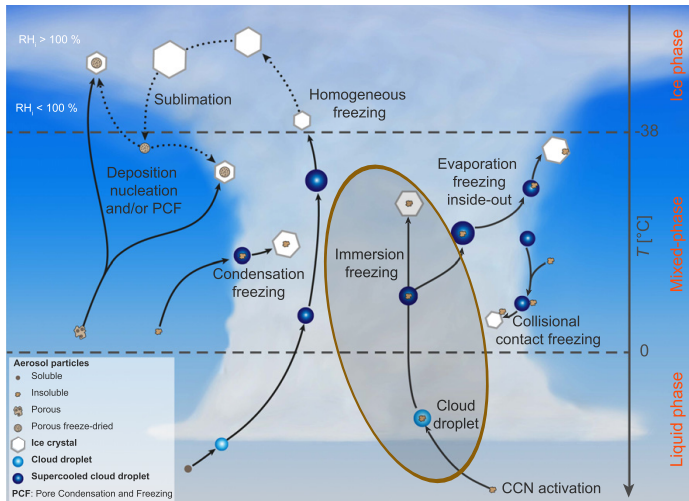
Vonnegut 1948 (J. Colloid Sci.)



Fraction of water drops remaining unfrozen as a function of time.

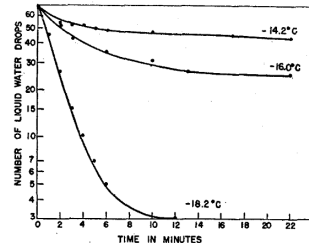
Kanji et al. 2017, graphics F. Mahrt, <https://doi.org/10.1175/AMSMONOGRAPHS-D-16-0006.1>

immersion freezing and other ice crystal formation pathways in clouds



Kanji et al. 2017, graphics F. Mahrt, <https://doi.org/10.1175/AMSMONOGRAPHS-D-16-0006.1>

Vonnegut 1948 (J. Colloid Sci.)



Fraction of water drops remaining unfrozen as a function of time.

Vali 2014 (ACP)

"Interpretations of the experimental results face considerable difficulties ... two separate ways of interpreting the same observations; one assigned primacy to time the other emphasized the temperature-dependent impacts of the impurities ... dichotomy – the stochastic and singular models"

Heterogeneous Nucleations is a Stochastic Process

by

J. S. MARSHALL

McGill University, Montreal, Canad.

*Presented at the International Congress on the Physics of Clouds (Hailstorms)
at Verona 9-13 August 1960.*

http://cma.entecra.it/Astro2_sito/doc/Nubila_1_1961.pdf

Poissonian model of freezing & Ice Nucleation Active Sites (INAS)

theory (in modern notation)

(Bigg '53, Langham & Mason '58, Carte '59, Marshall '61)

Poissonian model of freezing & Ice Nucleation Active Sites (INAS)

theory (in modern notation)

(Bigg '53, Langham & Mason '58, Carte '59, Marshall '61)

Poisson counting process with rate r :

$$P^*(k \text{ events in time } t) = \frac{(rt)^k \exp(-rt)}{k!}$$

$$P(\text{one or more events in time } t) = 1 - P^*(k = 0, t)$$

$$\ln(1 - P) = -rt$$

Poissonian model of freezing & Ice Nucleation Active Sites (INAS)

theory (in modern notation)

(Bigg '53, Langham & Mason '58, Carte '59, Marshall '61)

Poisson counting process with rate r :

$$P^*(k \text{ events in time } t) = \frac{(rt)^k \exp(-rt)}{k!}$$

$$P(\text{one or more events in time } t) = 1 - P^*(k = 0, t)$$

$$\ln(1 - P) = -rt$$

introducing $J_{\text{het}}(T)$, $T(t)$ and INP surface A :

$$\ln(1 - P(A, t)) = -A \underbrace{\int_0^t J_{\text{het}}(T(t')) dt'}_{I(T)}$$

Poissonian model of freezing & Ice Nucleation Active Sites (INAS)

theory (in modern notation)

(Bigg '53, Langham & Mason '58, Carte '59, Marshall '61)

Poisson counting process with rate r :

$$P^*(k \text{ events in time } t) = \frac{(rt)^k \exp(-rt)}{k!}$$

$$P(\text{one or more events in time } t) = 1 - P^*(k = 0, t)$$

$$\ln(1 - P) = -rt$$

introducing $J_{\text{het}}(T)$, $T(t)$ and INP surface A :

$$\ln(1 - P(A, t)) = -A \underbrace{\int_0^t J_{\text{het}}(T(t')) dt'}_{I(T)}$$

INAS: $I(T) = n_s(T) = \exp(a \cdot (T - T_0^{\circ\text{C}}) + b)$

Poissonian model of freezing & Ice Nucleation Active Sites (INAS)

theory (in modern notation)

(Bigg '53, Langham & Mason '58, Carte '59, Marshall '61)

Poisson counting process with rate r :

$$P^*(k \text{ events in time } t) = \frac{(rt)^k \exp(-rt)}{k!}$$

$$P(\text{one or more events in time } t) = 1 - P^*(k = 0, t)$$

$$\ln(1 - P) = -rt$$

introducing $J_{\text{het}}(T)$, $T(t)$ and INP surface A :

$$\ln(1 - P(A, t)) = -A \underbrace{\int_0^t J_{\text{het}}(T(t')) dt'}_{I(T)}$$

INAS: $I(T) = n_s(T) = \exp(a \cdot (T - T_0^\circ\text{C}) + b)$

experimental $n_s(T)$ fits: e.g., Niemand et al. 2012

freezing temperature T_{fz} as a super-particle attribute

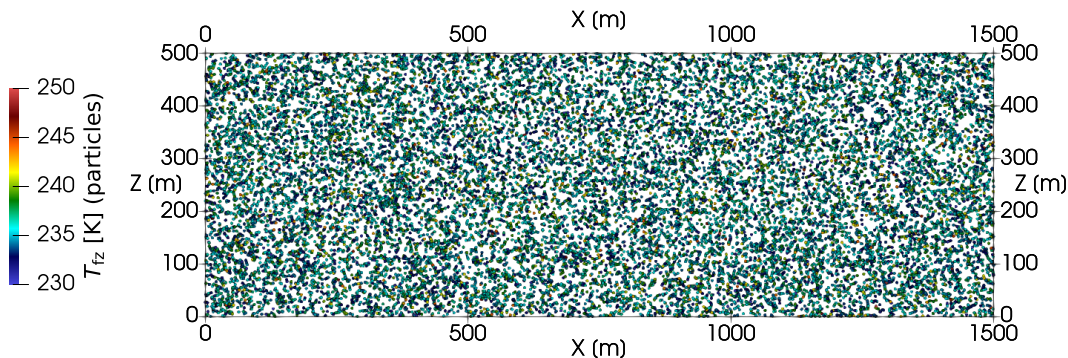
$$P(A, T_{fz}) = 1 - \exp(-A \cdot n_s(T_{fz}))$$

spectrum of T_{fz} even for monodisperse A

freezing temperature T_{fz} as a super-particle attribute

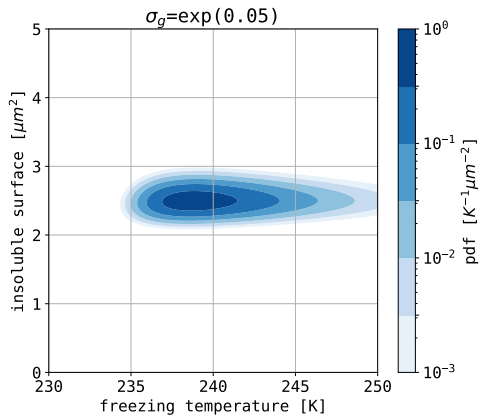
$$P(A, T_{fz}) = 1 - \exp(-A \cdot n_s(T_{fz}))$$

spectrum of T_{fz} even for monodisperse A



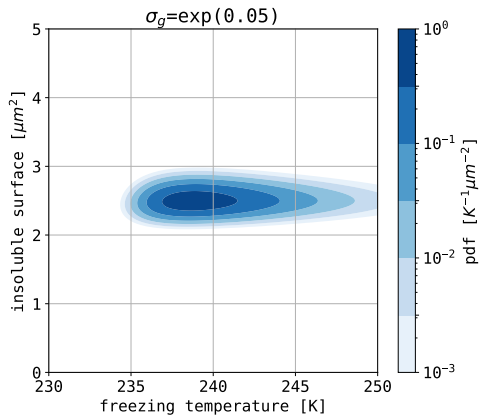
freezing temperature T_{fz} as a super-particle attribute: initialisation

INAS $P(T_{fz}, A)$ sampling (A lognormal)



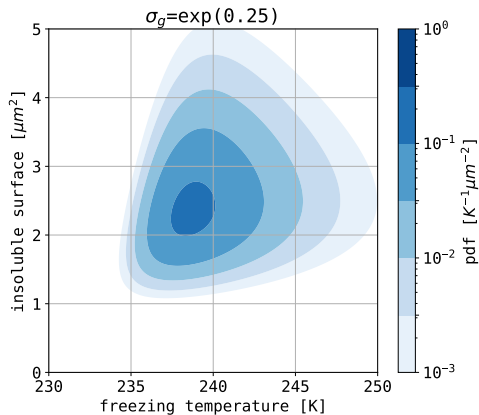
freezing temperature T_{fz} as a super-particle attribute: initialisation

INAS $P(T_{fz}, A)$ sampling (A lognormal)



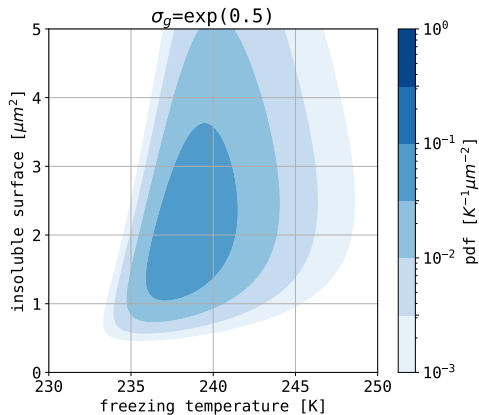
freezing temperature T_{fz} as a super-particle attribute: initialisation

INAS P(T_{fz}, A) sampling (A lognormal)



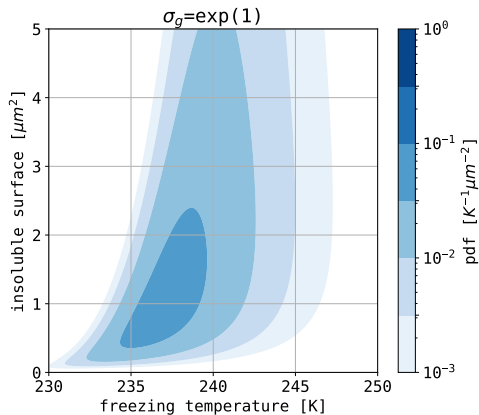
freezing temperature T_{fz} as a super-particle attribute: initialisation

INAS P(T_{fz}, A) sampling (A lognormal)



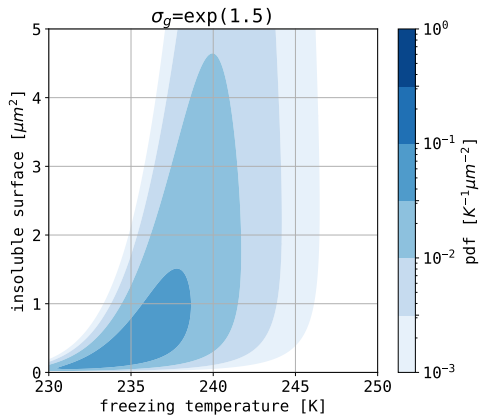
freezing temperature T_{fz} as a super-particle attribute: initialisation

INAS $P(T_{fz}, A)$ sampling (A lognormal)



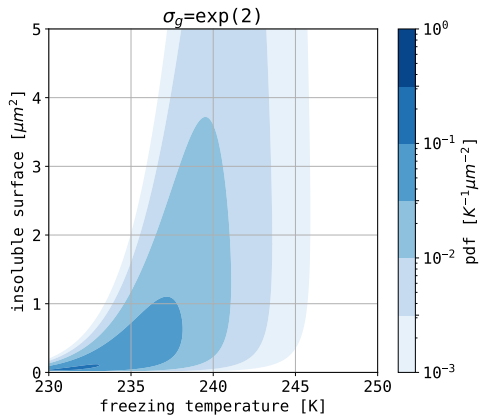
freezing temperature T_{fz} as a super-particle attribute: initialisation

INAS $P(T_{fz}, A)$ sampling (A lognormal)



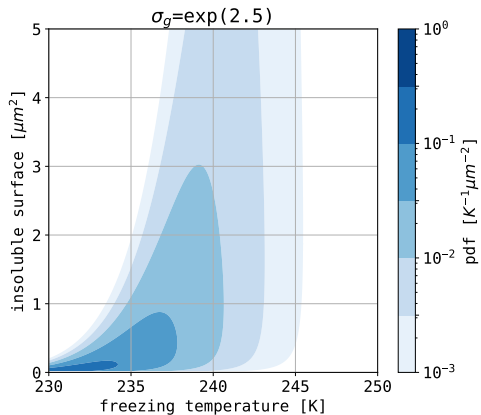
freezing temperature T_{fz} as a super-particle attribute: initialisation

INAS $P(T_{fz}, A)$ sampling (A lognormal)



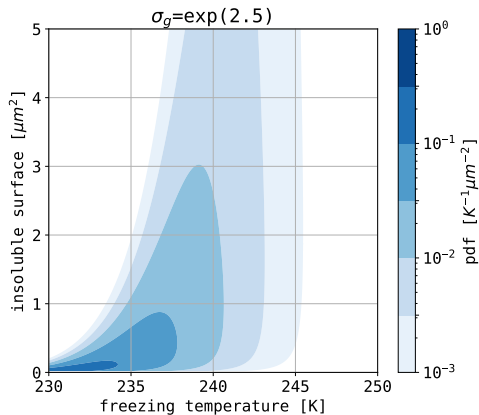
freezing temperature T_{fz} as a super-particle attribute: initialisation

INAS $P(T_{fz}, A)$ sampling (A lognormal)

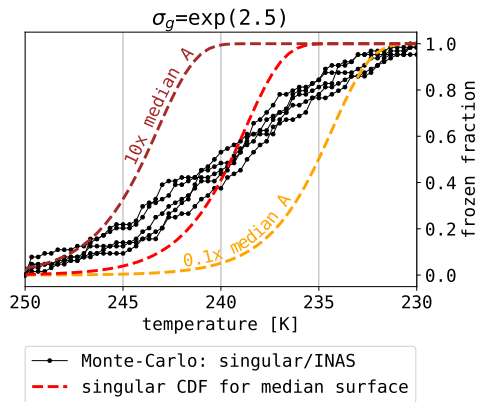


freezing temperature T_{fz} as a super-particle attribute: initialisation

INAS $P(T_{fz}, A)$ sampling (A lognormal)



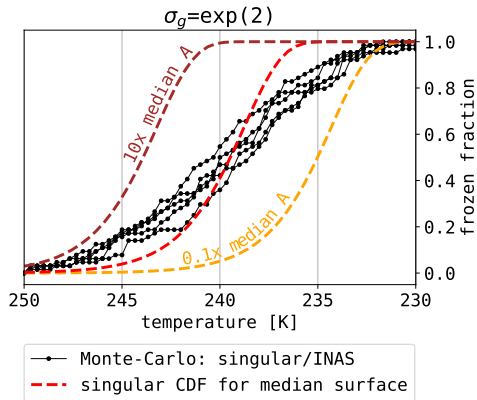
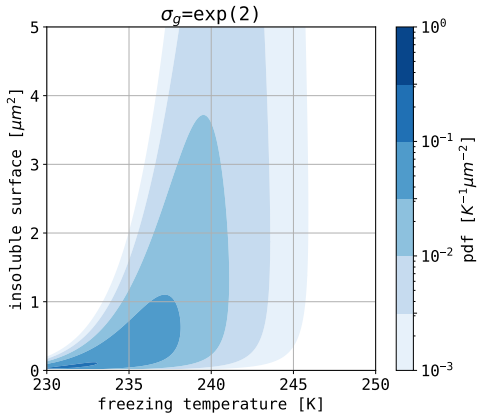
box model (or single grid cell)



freezing temperature T_{fz} as a super-particle attribute: initialisation

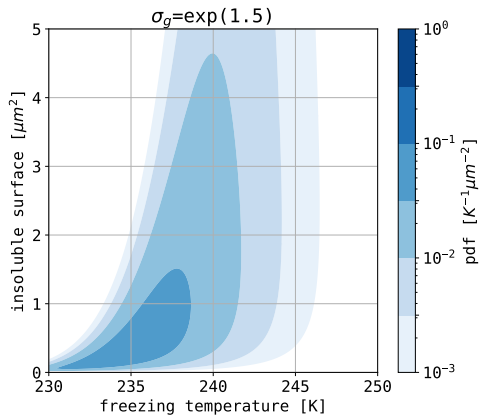
INAS $P(T_{fz}, A)$ sampling (A lognormal)

box model (or single grid cell)

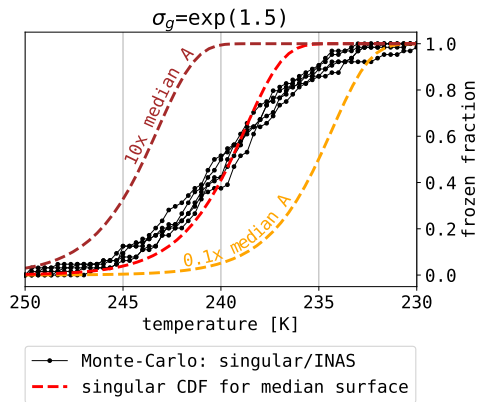


freezing temperature T_{fz} as a super-particle attribute: initialisation

INAS $P(T_{fz}, A)$ sampling (A lognormal)

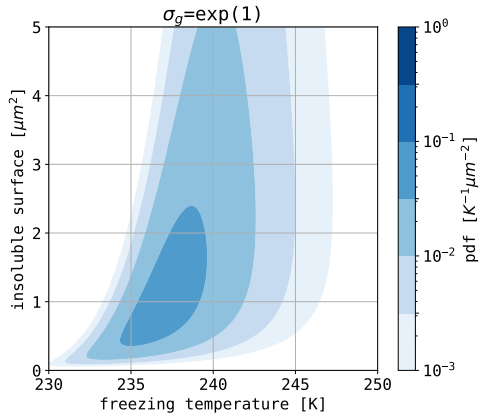


box model (or single grid cell)

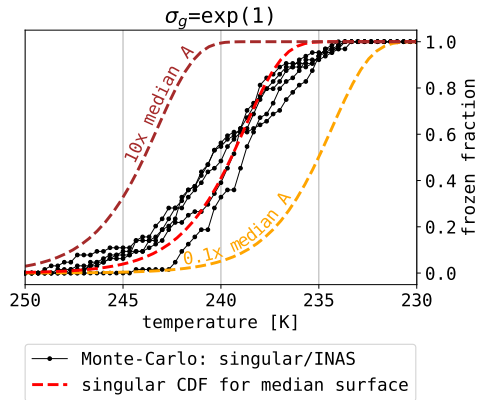


freezing temperature T_{fz} as a super-particle attribute: initialisation

INAS $P(T_{fz}, A)$ sampling (A lognormal)

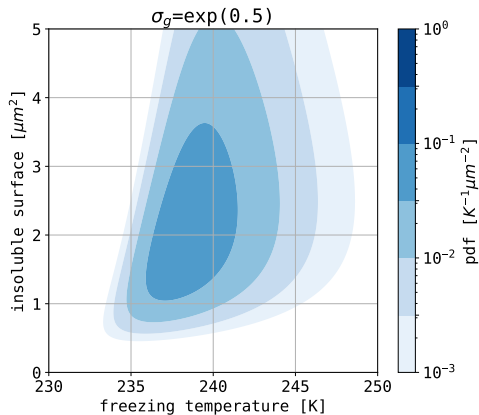


box model (or single grid cell)

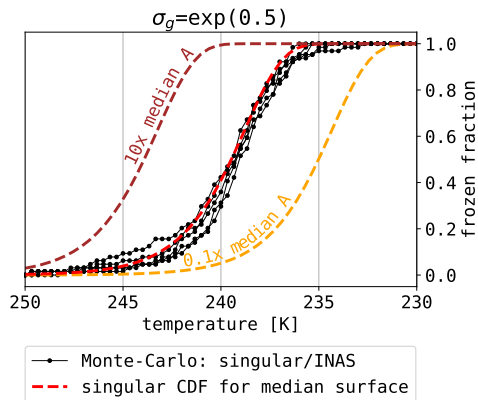


freezing temperature T_{fz} as a super-particle attribute: initialisation

INAS $P(T_{fz}, A)$ sampling (A lognormal)

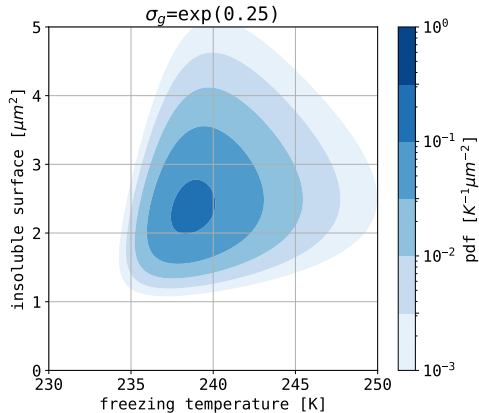


box model (or single grid cell)

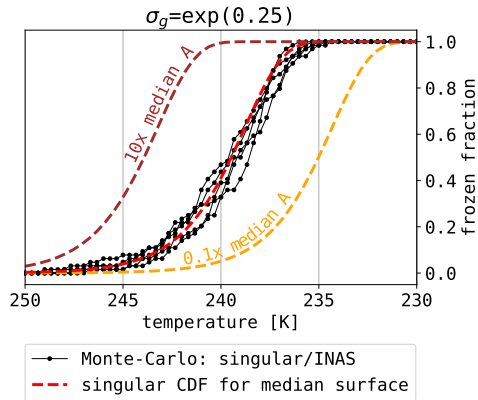


freezing temperature T_{fz} as a super-particle attribute: initialisation

INAS $P(T_{fz}, A)$ sampling (A lognormal)

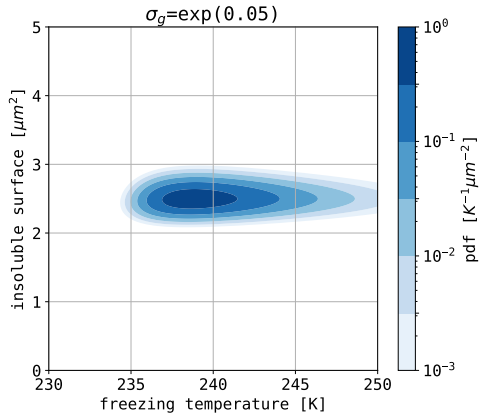


box model (or single grid cell)

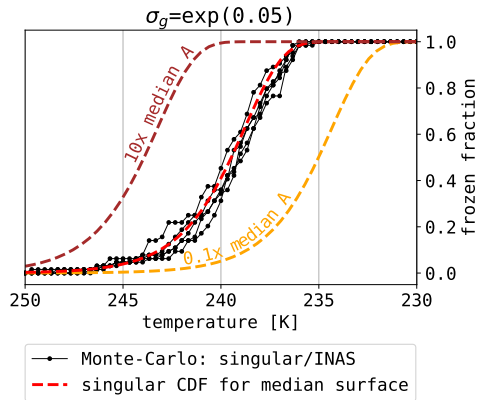


freezing temperature T_{fz} as a super-particle attribute: initialisation

INAS $P(T_{fz}, A)$ sampling (A lognormal)

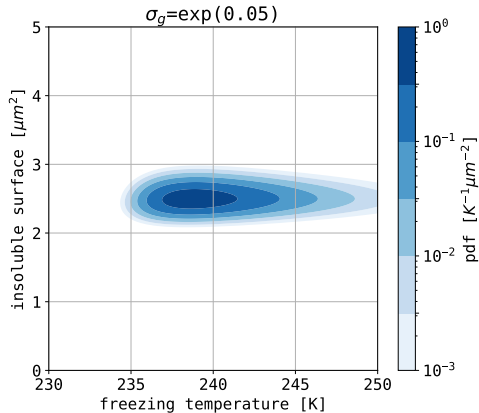


box model (or single grid cell)

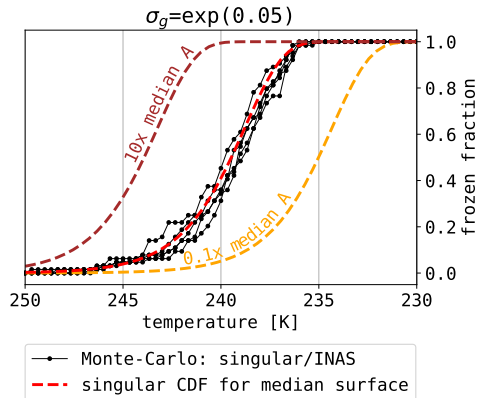


freezing temperature T_{fz} as a super-particle attribute: initialisation

INAS $P(T_{fz}, A)$ sampling (A lognormal)



box model (or single grid cell)

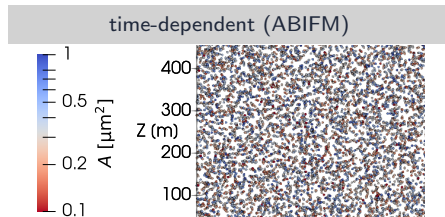
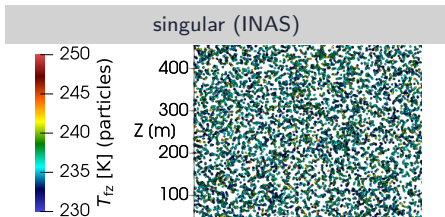


- “singular” particle-based model is capable of representing polydisperse INP
- depicted limitations stemming from monodisperse INP assumption

particle-based freezing: singular (Shima et al.) / time-dependent (this work)

singular: INAS T_{fz} as **attribute**; initialisation by random sampling from $P(T_{fz}, A)$ with lognormal A (A is not an attribute, initialisation only); freezing if $T(t) < T_{fz}(t = 0)$

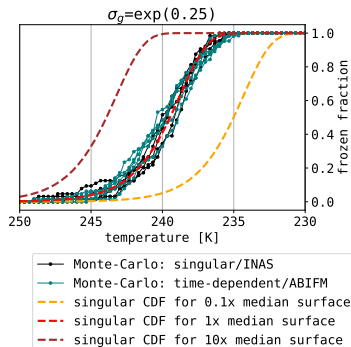
time-dependent: A as **attribute** (randomly sampled from the same lognormal)
Monte-Carlo freezing trigger using $P(J_{het}(T(t)))$



particle-based freezing: singular (Shima et al.) / time-dependent (this work)

singular: INAS T_{fz} as **attribute**; initialisation by random sampling from $P(T_{fz}, A)$ with lognormal A (A is not an attribute, initialisation only); freezing if $T(t) < T_{fz}(t = 0)$

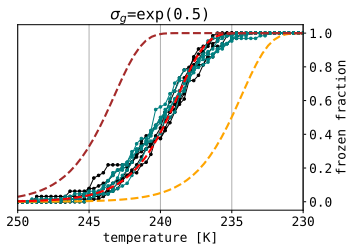
time-dependent: A as **attribute** (randomly sampled from the same lognormal)
Monte-Carlo freezing trigger using $P(J_{het}(T(t)))$



particle-based freezing: singular (Shima et al.) / time-dependent (this work)

singular: INAS T_{fz} as **attribute**; initialisation by random sampling from $P(T_{fz}, A)$ with lognormal A (A is not an attribute, initialisation only); freezing if $T(t) < T_{fz}(t = 0)$

time-dependent: A as **attribute** (randomly sampled from the same lognormal)
Monte-Carlo freezing trigger using $P(J_{het}(T(t)))$

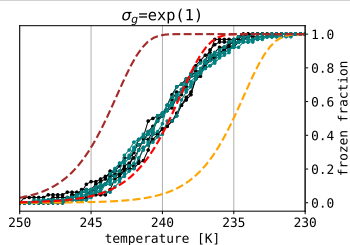


—•— Monte-Carlo: singular/INAS
—•— Monte-Carlo: time-dependent/ABIFM
- - - singular CDF for 0.1x median surface
- - - singular CDF for 1x median surface
- - - singular CDF for 10x median surface

particle-based freezing: singular (Shima et al.) / time-dependent (this work)

singular: INAS T_{fz} as **attribute**; initialisation by random sampling from $P(T_{fz}, A)$ with lognormal A (A is not an attribute, initialisation only); freezing if $T(t) < T_{fz}(t = 0)$

time-dependent: A as **attribute** (randomly sampled from the same lognormal)
Monte-Carlo freezing trigger using $P(J_{het}(T(t)))$

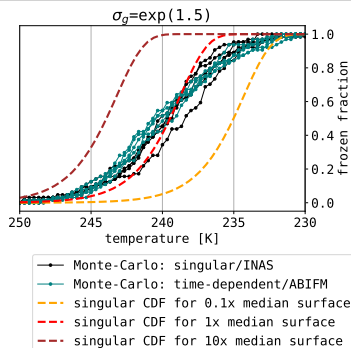


- Monte-Carlo: singular/INAS
- Monte-Carlo: time-dependent/ABIFM
- - - singular CDF for 0.1x median surface
- - - singular CDF for 1x median surface
- - - singular CDF for 10x median surface

particle-based freezing: singular (Shima et al.) / time-dependent (this work)

singular: INAS T_{fz} as **attribute**; initialisation by random sampling from $P(T_{fz}, A)$ with lognormal A (A is not an attribute, initialisation only); freezing if $T(t) < T_{fz}(t = 0)$

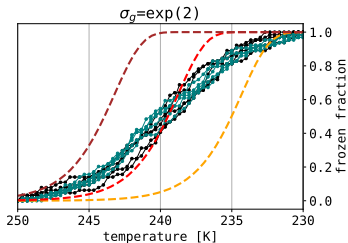
time-dependent: A as **attribute** (randomly sampled from the same lognormal)
Monte-Carlo freezing trigger using $P(J_{het}(T(t)))$



particle-based freezing: singular (Shima et al.) / time-dependent (this work)

singular: INAS T_{fz} as **attribute**; initialisation by random sampling from $P(T_{fz}, A)$ with lognormal A (A is not an attribute, initialisation only); freezing if $T(t) < T_{fz}(t = 0)$

time-dependent: A as **attribute** (randomly sampled from the same lognormal)
Monte-Carlo freezing trigger using $P(J_{het}(T(t)))$

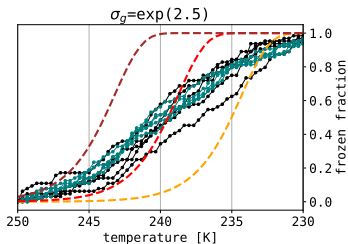


- Monte-Carlo: singular/INAS
- Monte-Carlo: time-dependent/ABIFM
- - - singular CDF for 0.1x median surface
- - - singular CDF for 1x median surface
- - - singular CDF for 10x median surface

particle-based freezing: singular (Shima et al.) / time-dependent (this work)

singular: INAS T_{fz} as **attribute**; initialisation by random sampling from $P(T_{fz}, A)$ with lognormal A (A is not an attribute, initialisation only); freezing if $T(t) < T_{fz}(t = 0)$

time-dependent: A as **attribute** (randomly sampled from the same lognormal)
Monte-Carlo freezing trigger using $P(J_{het}(T(t)))$



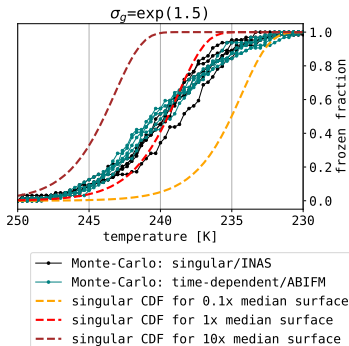
—●— Monte-Carlo: singular/INAS
—●— Monte-Carlo: time-dependent/ABIFM
- - - singular CDF for 0.1x median surface
- - - singular CDF for 1x median surface
- - - singular CDF for 10x median surface

particle-based freezing: singular (Shima et al.) / time-dependent (this work)

singular: INAS T_{fz} as **attribute**; initialisation by random sampling from $P(T_{fz}, A)$ with lognormal A (A is not an attribute, initialisation only); freezing if $T(t) < T_{fz}(t = 0)$

time-dependent: A as **attribute** (randomly sampled from the same lognormal)
Monte-Carlo freezing trigger using $P(J_{het}(T(t)))$

cooling rate: $0.5 \text{ K}/\text{min}$

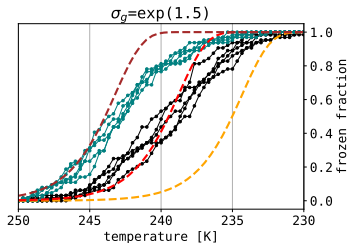


particle-based freezing: singular (Shima et al.) / time-dependent (this work)

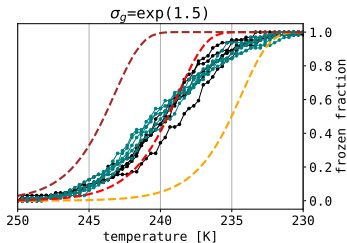
singular: INAS T_{fz} as **attribute**; initialisation by random sampling from $P(T_{fz}, A)$ with lognormal A (A is not an attribute, initialisation only); freezing if $T(t) < T_{fz}(t = 0)$

time-dependent: A as **attribute** (randomly sampled from the same lognormal)
Monte-Carlo freezing trigger using $P(J_{het}(T(t)))$

cooling rate: $0.1 \text{ K}/\text{min}$



cooling rate: $0.5 \text{ K}/\text{min}$



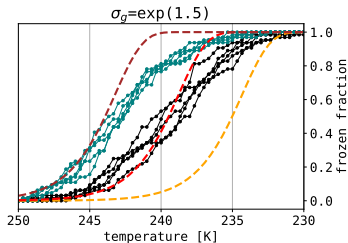
—●— Monte-Carlo: singular/INAS
—●— Monte-Carlo: time-dependent/ABIFM
- - - singular CDF for 0.1x median surface
- - - singular CDF for 1x median surface
- - - singular CDF for 10x median surface

particle-based freezing: singular (Shima et al.) / time-dependent (this work)

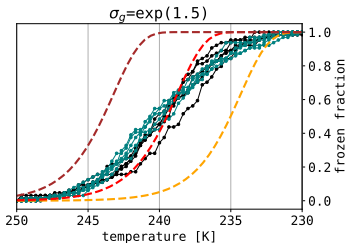
singular: INAS T_{fz} as **attribute**; initialisation by random sampling from $P(T_{fz}, A)$ with lognormal A (A is not an attribute, initialisation only); freezing if $T(t) < T_{fz}(t = 0)$

time-dependent: A as **attribute** (randomly sampled from the same lognormal)
Monte-Carlo freezing trigger using $P(J_{het}(T(t)))$

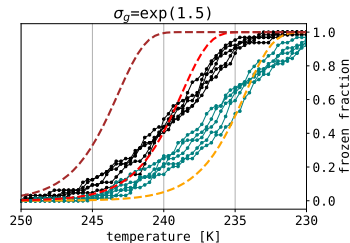
cooling rate: 0.1 K/min



cooling rate: 0.5 K/min



cooling rate: 2.5 K/min



—●— Monte-Carlo: singular/INAS
—●— Monte-Carlo: time-dependent/ABIFM
—●— singular CDF for 0.1x median surface
—●— singular CDF for 1x median surface
—●— singular CDF for 10x median surface

Poissonian model of freezing & Ice Nucleation Active Sites (INAS)

theory (in modern notation)

(Bigg '53, Langham & Mason '58, Carte '59, Marshall '61)

Poisson counting process with rate r :

$$P^*(k \text{ events in time } t) = \frac{(rt)^k \exp(-rt)}{k!}$$

$$P(\text{one or more events in time } t) = 1 - P^*(k = 0, t)$$

$$\ln(1 - P) = -rt$$

introducing $J_{\text{het}}(T)$, $T(t)$ and INP surface A :

$$\ln(1 - P(A, t)) = -A \underbrace{\int_0^t J_{\text{het}}(T(t')) dt'}_{I(T)}$$

INAS: $I(T) = n_s(T) = \exp(a \cdot (T - T_{0^\circ\text{C}}) + b)$

experimental $n_s(T)$ fits: e.g., Niemand et al. 2012

for a constant cooling rate $c = dT/dt$:

$$\ln(1 - P(A, t)) = -\frac{A}{c} \int_{T_0}^{T_0+ct} J_{\text{het}}(T') dT' = -A \cdot I(T)$$

Poissonian model of freezing & Ice Nucleation Active Sites (INAS)

theory (in modern notation)

(Bigg '53, Langham & Mason '58, Carte '59, Marshall '61)

Poisson counting process with rate r :

$$P^*(k \text{ events in time } t) = \frac{(rt)^k \exp(-rt)}{k!}$$

$$P(\text{one or more events in time } t) = 1 - P^*(k = 0, t)$$

$$\ln(1 - P) = -rt$$

introducing $J_{\text{het}}(T)$, $T(t)$ and INP surface A :

$$\ln(1 - P(A, t)) = -A \underbrace{\int_0^t J_{\text{het}}(T(t')) dt'}_{I(T)}$$

INAS: $I(T) = n_s(T) = \exp(a \cdot (T - T_{0^\circ\text{C}}) + b)$

experimental $n_s(T)$ fits: e.g., Niemand et al. 2012

for a constant cooling rate $c = dT/dt$:

$$\ln(1 - P(A, t)) = -\frac{A}{c} \int_{T_0}^{T_0+ct} J_{\text{het}}(T') dT' = -A \cdot I(T)$$

$$\frac{dn_s(T)}{dT} = a \cdot n_s(T) = -\frac{1}{c} J_{\text{het}}(T)$$

Poissonian model of freezing & Ice Nucleation Active Sites (INAS)

theory (in modern notation)

(Bigg '53, Langham & Mason '58, Carte '59, Marshall '61)

Poisson counting process with rate r :

$$P^*(k \text{ events in time } t) = \frac{(rt)^k \exp(-rt)}{k!}$$

$$P(\text{one or more events in time } t) = 1 - P^*(k = 0, t)$$

$$\ln(1 - P) = -rt$$

introducing $J_{\text{het}}(T)$, $T(t)$ and INP surface A :

$$\ln(1 - P(A, t)) = -A \underbrace{\int_0^t J_{\text{het}}(T(t')) dt'}_{I(T)}$$

INAS: $I(T) = n_s(T) = \exp(a \cdot (T - T_{0^\circ\text{C}}) + b)$

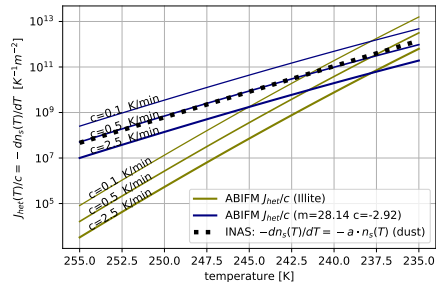
experimental $n_s(T)$ fits: e.g., Niemand et al. 2012

for a constant cooling rate $c = dT/dt$:

$$\ln(1 - P(A, t)) = -\frac{A}{c} \int_{T_0}^{T_0+ct} J_{\text{het}}(T') dT' = -A \cdot I(T)$$

$$\frac{dn_s(T)}{dT} = a \cdot n_s(T) = -\frac{1}{c} J_{\text{het}}(T)$$

experimental fits: INAS n_s (Niemand et al. '12)
ABIFM J_{het} (Knopf & Alpert '13)



Poissonian model of freezing & Ice Nucleation Active Sites (INAS)

theory (in modern notation)

(Bigg '53, Langham & Mason '58, Carte '59, Marshall '61)

Poisson counting process with rate r :

$$P^*(k \text{ events in time } t) = \frac{(rt)^k \exp(-rt)}{k!}$$

$$P(\text{one or more events in time } t) = 1 - P^*(k = 0, t)$$

$$\ln(1 - P) = -rt$$

introducing $J_{\text{het}}(T)$, $T(t)$ and INP surface A :

$$\ln(1 - P(A, t)) = -A \underbrace{\int_0^t J_{\text{het}}(T(t')) dt'}_{I(T)}$$

INAS: $I(T) = n_s(T) = \exp(a \cdot (T - T_0^\circ\text{C}) + b)$

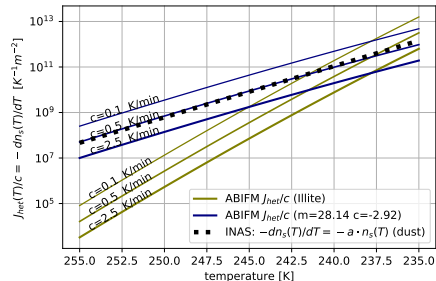
experimental $n_s(T)$ fits: e.g., Niemand et al. 2012

for a constant cooling rate $c = dT/dt$:

$$\ln(1 - P(A, t)) = -\frac{A}{c} \int_{T_0}^{T_0+ct} J_{\text{het}}(T') dT' = -A \cdot I(T)$$

$$\frac{dn_s(T)}{dT} = a \cdot n_s(T) = -\frac{1}{c} J_{\text{het}}(T)$$

experimental fits: INAS n_s (Niemand et al. '12)
ABIFM J_{het} (Knopf & Alpert '13)



cf. Vali & Stansbury '66; modified singular model (Vali '94, Murray et al. '11)
but the **singular ansatz limitation of sampling T_{fz} at $t=0$** remains

Poissonian model of freezing & Ice Nucleation Active Sites (INAS)

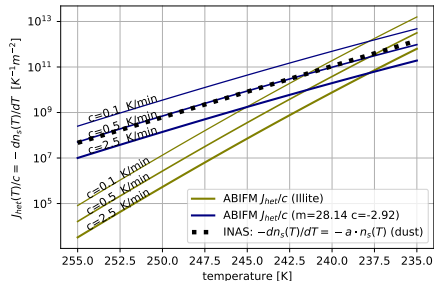
for a constant cooling rate $c = dT/dt$:

$$\ln(1 - P(A, t)) = -\frac{A}{c} \int_{T_0}^{T_0+ct} J_{\text{het}}(T') dT' = -A \cdot I(T)$$

$$\frac{dn_s(T)}{dT} = a \cdot n_s(T) = -\frac{1}{c} J_{\text{het}}(T)$$

experimental fits: INAS n_s (Niemand et al. '12)
 ABIFM J_{het} (Knopf & Alpert '13)

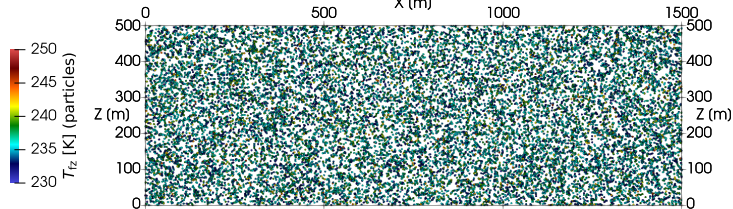
Is it a problem?



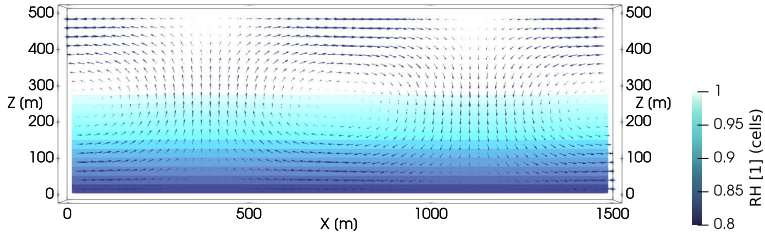
cf. Vali & Stansbury '66; modified singular model (Vali '94, Murray et al. '11)
 but the **singular ansatz limitation of sampling T_{fz} at $t=0$** remains

particle-based μ -physics + prescribed-flow test (aka KiD-2D)^{a,b,c,d,e}

Lagrangian component (PySDM)



Eulerian component (PyMPDATA)



• **concept:** Gedzelman & Arnold '93

• **stratiform:** Morrison & Grabowski '07

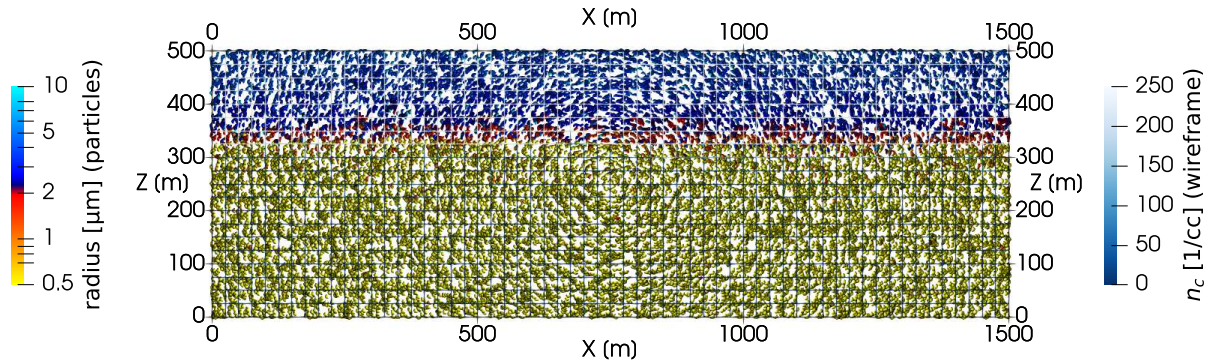
• **particle-based:** Arabas et al. '15

• **KiD-2D:** github.com/BShipway/KiD

• **here:** SHEBA case (Fridlind et al. '12)

particle-based μ -physics + prescribed-flow test

Time: 30 s (spin-up till 600.0 s)



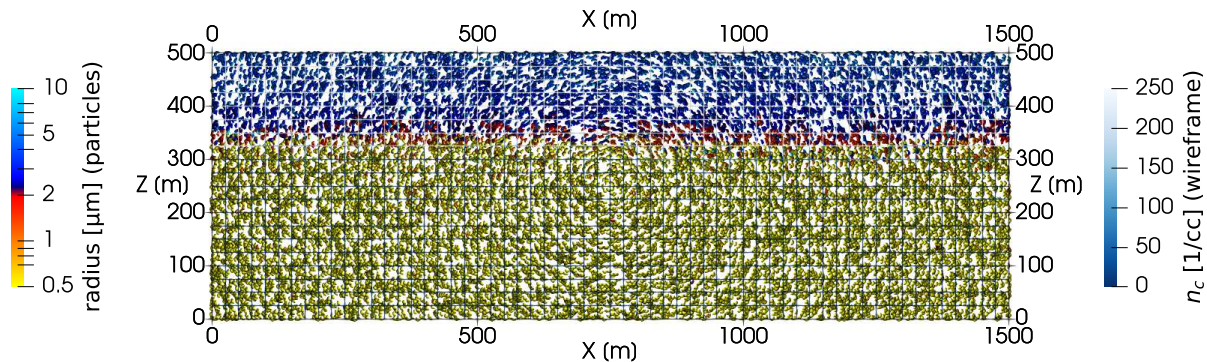
16+16 super-particles/cell for INP-rich + INP-free particles

$N_{\text{aer}} = 300/\text{cc}$ (two-mode lognormal) $N_{\text{INP}} = 150/L$ (lognormal, $D_g = 0.74 \mu\text{m}$, $\sigma_g = 2.55$)

spin-up = freezing off; subsequently frozen particles act as tracers

particle-based μ -physics + prescribed-flow test

Time: 60 s (spin-up till 600.0 s)



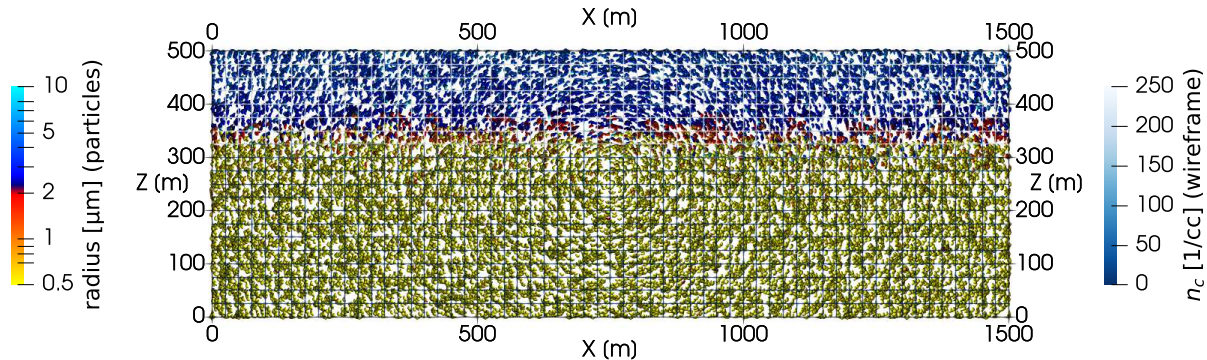
16+16 super-particles/cell for INP-rich + INP-free particles

$N_{\text{aer}} = 300/\text{cc}$ (two-mode lognormal) $N_{\text{INP}} = 150/L$ (lognormal, $D_g = 0.74 \mu\text{m}$, $\sigma_g = 2.55$)

spin-up = freezing off; subsequently frozen particles act as tracers

particle-based μ -physics + prescribed-flow test

Time: 90 s (spin-up till 600.0 s)



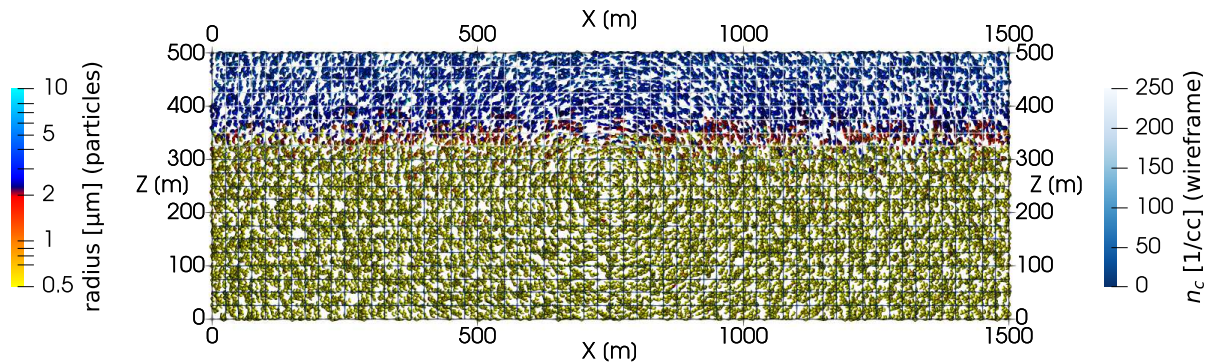
16+16 super-particles/cell for INP-rich + INP-free particles

$N_{\text{aer}} = 300/\text{cc}$ (two-mode lognormal) $N_{\text{INP}} = 150/L$ (lognormal, $D_g = 0.74 \mu\text{m}$, $\sigma_g = 2.55$)

spin-up = freezing off; subsequently frozen particles act as tracers

particle-based μ -physics + prescribed-flow test

Time: 120 s (spin-up till 600.0 s)



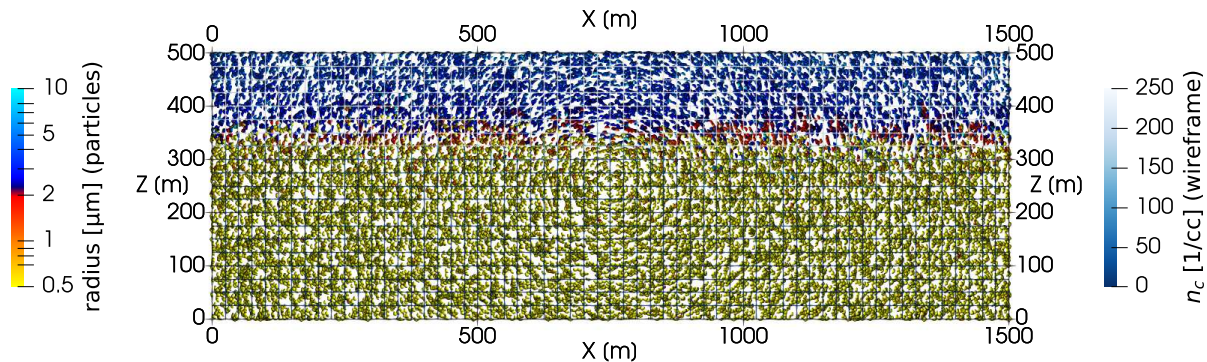
16+16 super-particles/cell for INP-rich + INP-free particles

$N_{\text{aer}} = 300/\text{cc}$ (two-mode lognormal) $N_{\text{INP}} = 150/L$ (lognormal, $D_g = 0.74 \mu\text{m}$, $\sigma_g = 2.55$)

spin-up = freezing off; subsequently frozen particles act as tracers

particle-based μ -physics + prescribed-flow test

Time: 150 s (spin-up till 600.0 s)



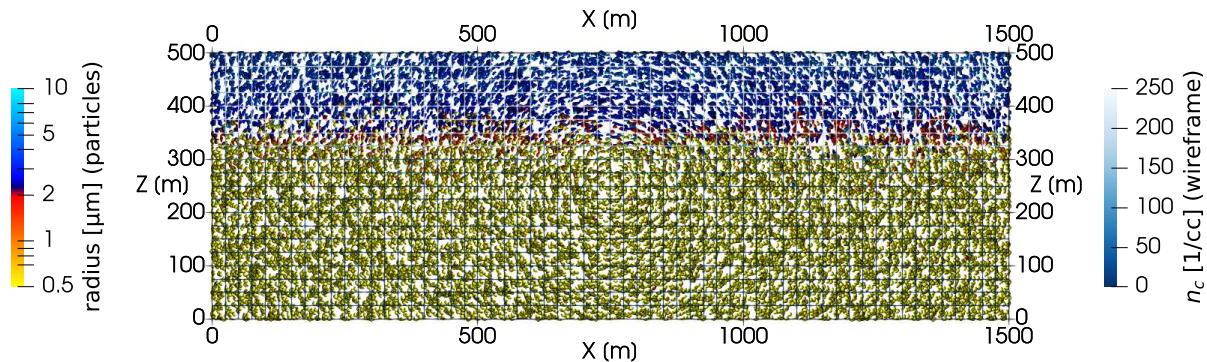
16+16 super-particles/cell for INP-rich + INP-free particles

$N_{\text{aer}} = 300/\text{cc}$ (two-mode lognormal) $N_{\text{INP}} = 150/L$ (lognormal, $D_g = 0.74 \mu\text{m}$, $\sigma_g = 2.55$)

spin-up = freezing off; subsequently frozen particles act as tracers

particle-based μ -physics + prescribed-flow test

Time: 180 s (spin-up till 600.0 s)



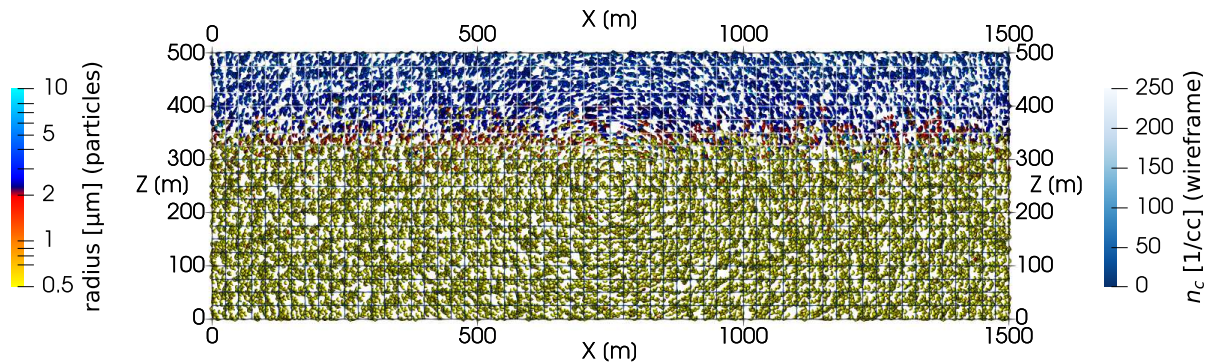
16+16 super-particles/cell for INP-rich + INP-free particles

$N_{\text{aer}} = 300/\text{cc}$ (two-mode lognormal) $N_{\text{INP}} = 150/L$ (lognormal, $D_g = 0.74 \mu\text{m}$, $\sigma_g = 2.55$)

spin-up = freezing off; subsequently frozen particles act as tracers

particle-based μ -physics + prescribed-flow test

Time: 210 s (spin-up till 600.0 s)



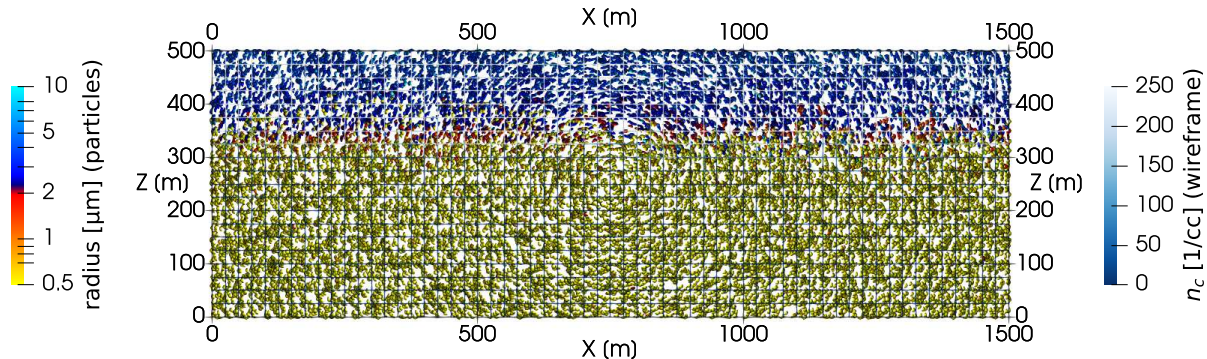
16+16 super-particles/cell for INP-rich + INP-free particles

$N_{\text{aer}} = 300/\text{cc}$ (two-mode lognormal) $N_{\text{INP}} = 150/L$ (lognormal, $D_g = 0.74 \mu\text{m}$, $\sigma_g = 2.55$)

spin-up = freezing off; subsequently frozen particles act as tracers

particle-based μ -physics + prescribed-flow test

Time: 240 s (spin-up till 600.0 s)



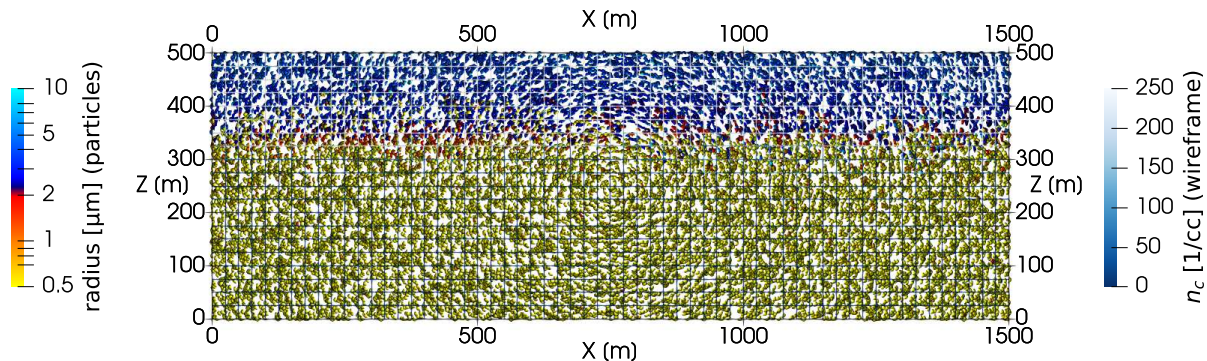
16+16 super-particles/cell for INP-rich + INP-free particles

$N_{\text{aer}} = 300/\text{cc}$ (two-mode lognormal) $N_{\text{INP}} = 150/L$ (lognormal, $D_g = 0.74 \mu\text{m}$, $\sigma_g = 2.55$)

spin-up = freezing off; subsequently frozen particles act as tracers

particle-based μ -physics + prescribed-flow test

Time: 270 s (spin-up till 600.0 s)



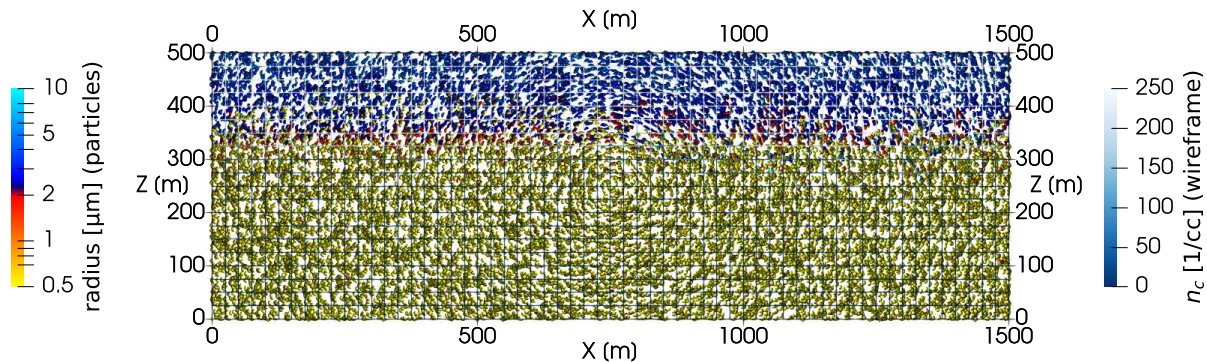
16+16 super-particles/cell for INP-rich + INP-free particles

$N_{\text{aer}} = 300/\text{cc}$ (two-mode lognormal) $N_{\text{INP}} = 150/L$ (lognormal, $D_g = 0.74 \mu\text{m}$, $\sigma_g = 2.55$)

spin-up = freezing off; subsequently frozen particles act as tracers

particle-based μ -physics + prescribed-flow test

Time: 300 s (spin-up till 600.0 s)



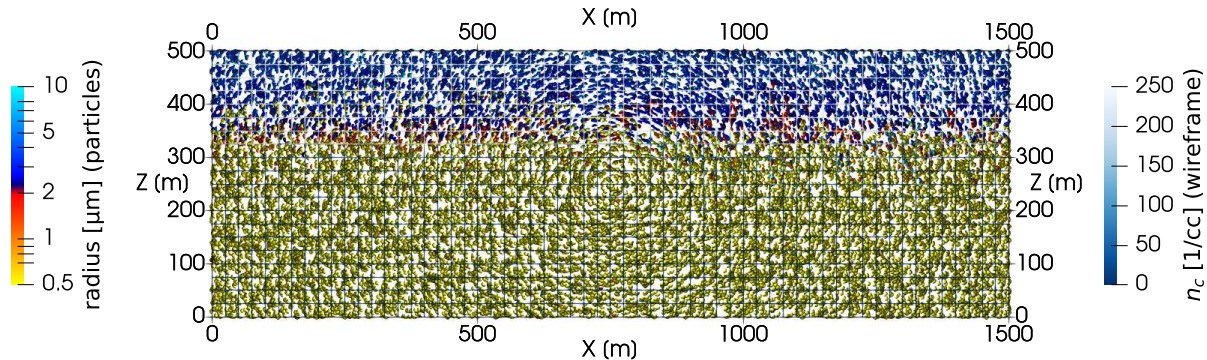
16+16 super-particles/cell for INP-rich + INP-free particles

$N_{\text{aer}} = 300/\text{cc}$ (two-mode lognormal) $N_{\text{INP}} = 150/L$ (lognormal, $D_g = 0.74 \mu\text{m}$, $\sigma_g = 2.55$)

spin-up = freezing off; subsequently frozen particles act as tracers

particle-based μ -physics + prescribed-flow test

Time: 330 s (spin-up till 600.0 s)



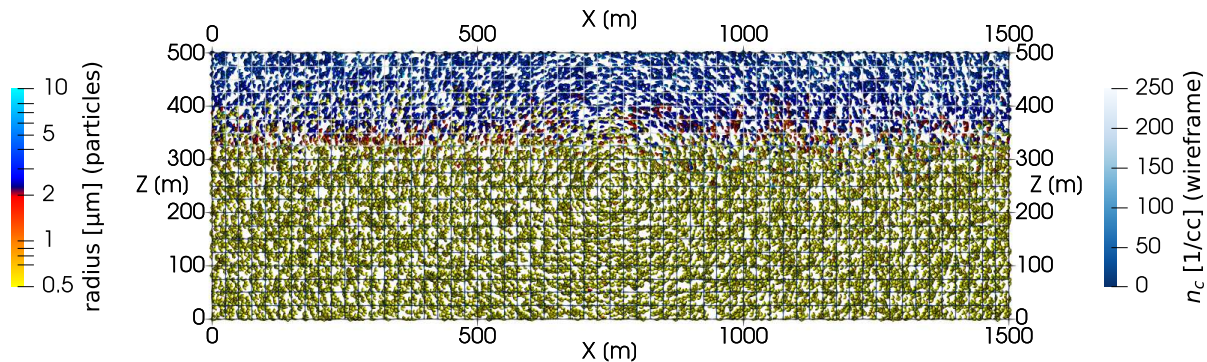
16+16 super-particles/cell for INP-rich + INP-free particles

$N_{\text{aer}} = 300/\text{cc}$ (two-mode lognormal) $N_{\text{INP}} = 150/L$ (lognormal, $D_g = 0.74 \mu\text{m}$, $\sigma_g = 2.55$)

spin-up = freezing off; subsequently frozen particles act as tracers

particle-based μ -physics + prescribed-flow test

Time: 360 s (spin-up till 600.0 s)



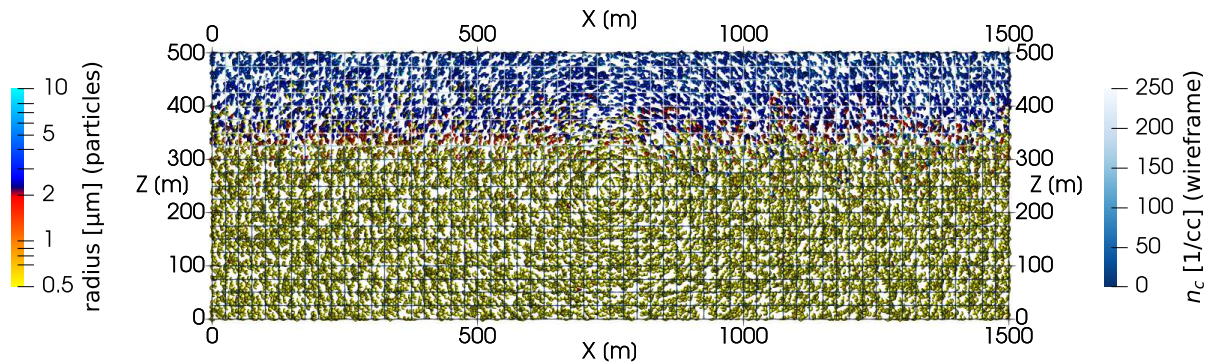
16+16 super-particles/cell for INP-rich + INP-free particles

$N_{\text{aer}} = 300/\text{cc}$ (two-mode lognormal) $N_{\text{INP}} = 150/L$ (lognormal, $D_g = 0.74 \mu\text{m}$, $\sigma_g = 2.55$)

spin-up = freezing off; subsequently frozen particles act as tracers

particle-based μ -physics + prescribed-flow test

Time: 390 s (spin-up till 600.0 s)



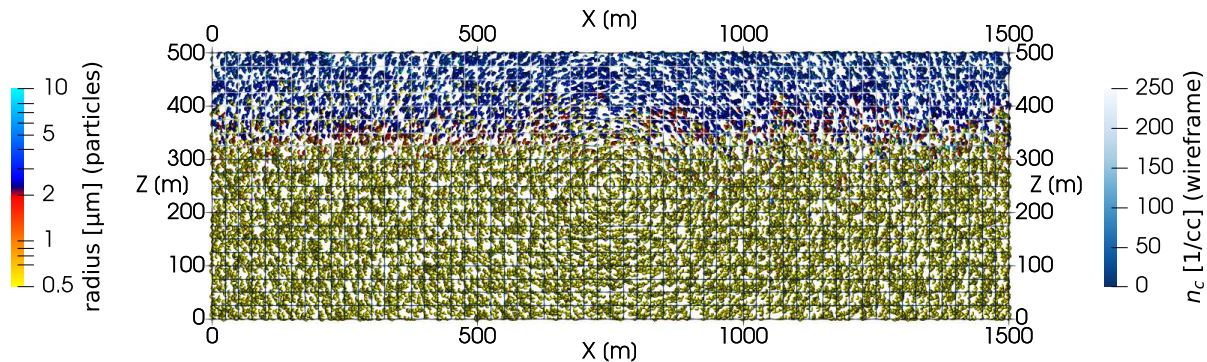
16+16 super-particles/cell for INP-rich + INP-free particles

$N_{\text{aer}} = 300/\text{cc}$ (two-mode lognormal) $N_{\text{INP}} = 150/L$ (lognormal, $D_g = 0.74 \mu\text{m}$, $\sigma_g = 2.55$)

spin-up = freezing off; subsequently frozen particles act as tracers

particle-based μ -physics + prescribed-flow test

Time: 420 s (spin-up till 600.0 s)



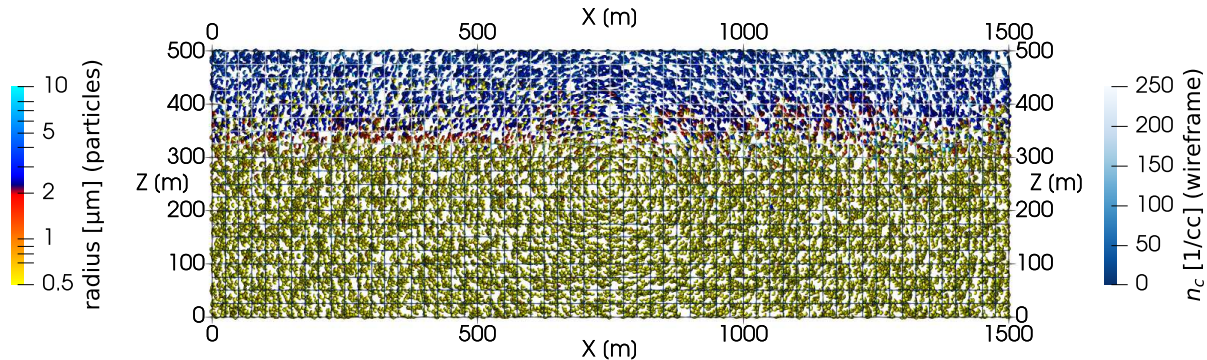
16+16 super-particles/cell for INP-rich + INP-free particles

$N_{\text{aer}} = 300/\text{cc}$ (two-mode lognormal) $N_{\text{INP}} = 150/L$ (lognormal, $D_g = 0.74 \mu\text{m}$, $\sigma_g = 2.55$)

spin-up = freezing off; subsequently frozen particles act as tracers

particle-based μ -physics + prescribed-flow test

Time: 450 s (spin-up till 600.0 s)



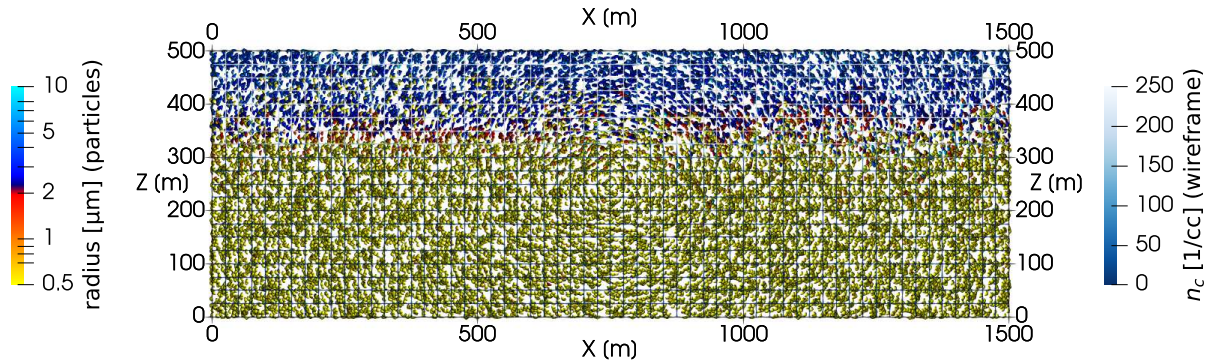
16+16 super-particles/cell for INP-rich + INP-free particles

$N_{\text{aer}} = 300/\text{cc}$ (two-mode lognormal) $N_{\text{INP}} = 150/L$ (lognormal, $D_g = 0.74 \mu\text{m}$, $\sigma_g = 2.55$)

spin-up = freezing off; subsequently frozen particles act as tracers

particle-based μ -physics + prescribed-flow test

Time: 480 s (spin-up till 600.0 s)



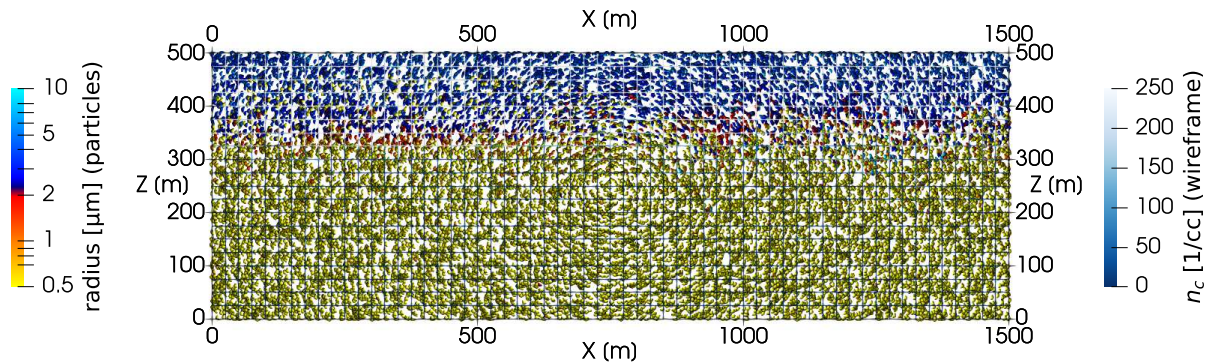
16+16 super-particles/cell for INP-rich + INP-free particles

$N_{\text{aer}} = 300/\text{cc}$ (two-mode lognormal) $N_{\text{INP}} = 150/L$ (lognormal, $D_g = 0.74 \mu\text{m}$, $\sigma_g = 2.55$)

spin-up = freezing off; subsequently frozen particles act as tracers

particle-based μ -physics + prescribed-flow test

Time: 510 s (spin-up till 600.0 s)



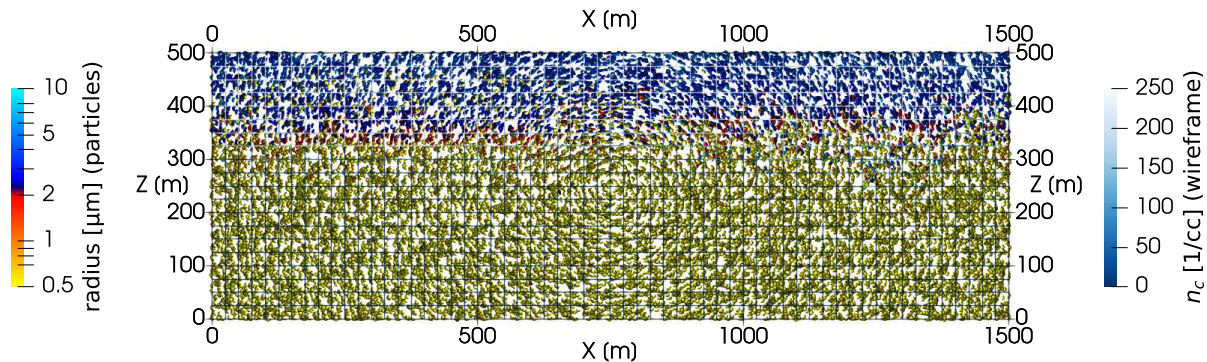
16+16 super-particles/cell for INP-rich + INP-free particles

$N_{\text{aer}} = 300/\text{cc}$ (two-mode lognormal) $N_{\text{INP}} = 150/L$ (lognormal, $D_g = 0.74 \mu\text{m}$, $\sigma_g = 2.55$)

spin-up = freezing off; subsequently frozen particles act as tracers

particle-based μ -physics + prescribed-flow test

Time: 540 s (spin-up till 600.0 s)



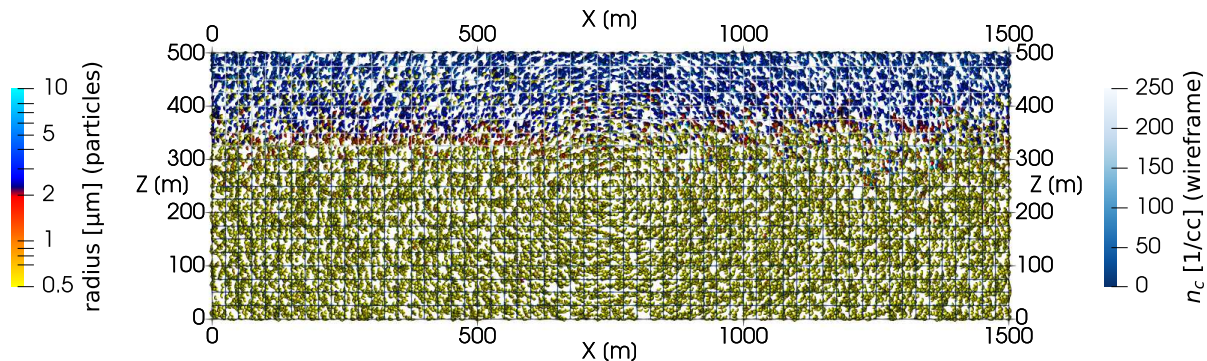
16+16 super-particles/cell for INP-rich + INP-free particles

$N_{\text{aer}} = 300/\text{cc}$ (two-mode lognormal) $N_{\text{INP}} = 150/L$ (lognormal, $D_g = 0.74 \mu\text{m}$, $\sigma_g = 2.55$)

spin-up = freezing off; subsequently frozen particles act as tracers

particle-based μ -physics + prescribed-flow test

Time: 570 s (spin-up till 600.0 s)



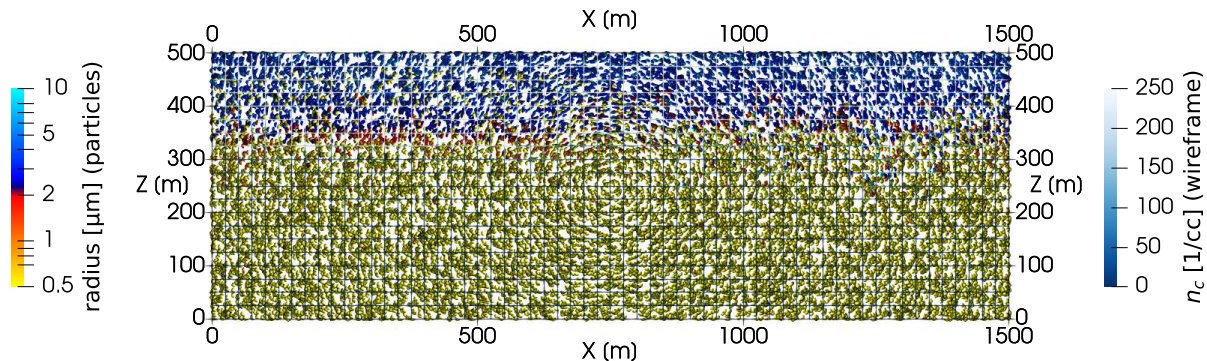
16+16 super-particles/cell for INP-rich + INP-free particles

$N_{\text{aer}} = 300/\text{cc}$ (two-mode lognormal) $N_{\text{INP}} = 150/L$ (lognormal, $D_g = 0.74 \mu\text{m}$, $\sigma_g = 2.55$)

spin-up = freezing off; subsequently frozen particles act as tracers

particle-based μ -physics + prescribed-flow test

Time: 600 s (spin-up till 600.0 s)



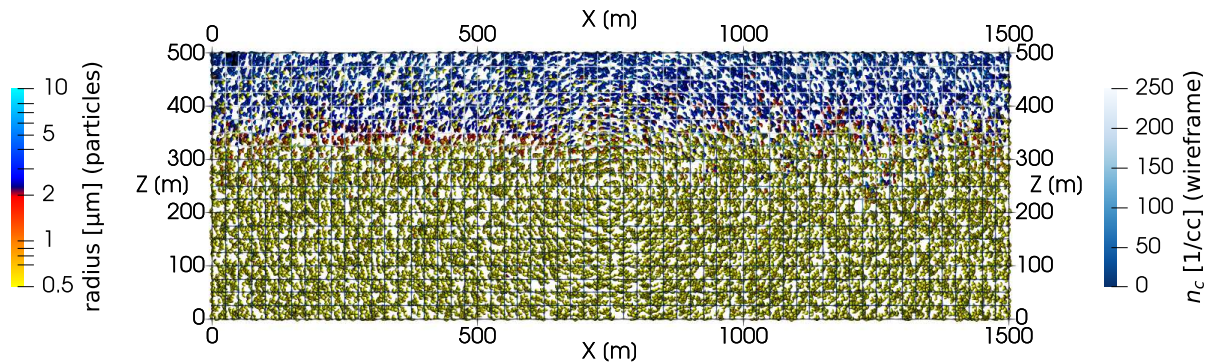
16+16 super-particles/cell for INP-rich + INP-free particles

$N_{\text{aer}} = 300/\text{cc}$ (two-mode lognormal) $N_{\text{INP}} = 150/L$ (lognormal, $D_g = 0.74 \mu\text{m}$, $\sigma_g = 2.55$)

spin-up = freezing off; subsequently frozen particles act as tracers

particle-based μ -physics + prescribed-flow test

Time: 630 s (spin-up till 600.0 s)



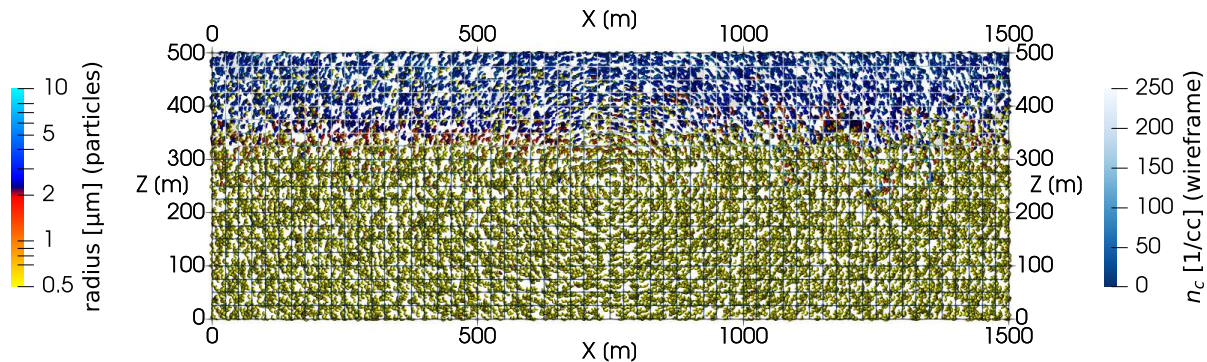
16+16 super-particles/cell for INP-rich + INP-free particles

$N_{\text{aer}} = 300/\text{cc}$ (two-mode lognormal) $N_{\text{INP}} = 150/L$ (lognormal, $D_g = 0.74 \mu\text{m}$, $\sigma_g = 2.55$)

spin-up = freezing off; subsequently frozen particles act as tracers

particle-based μ -physics + prescribed-flow test

Time: 660 s (spin-up till 600.0 s)



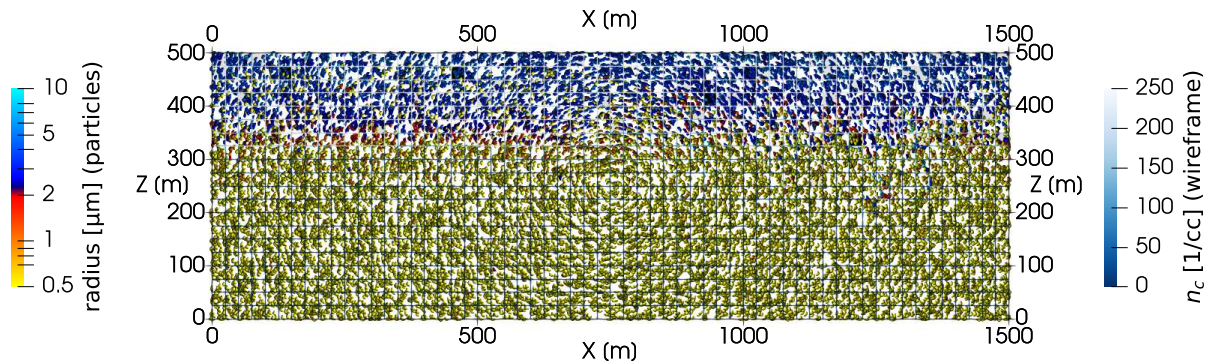
16+16 super-particles/cell for INP-rich + INP-free particles

$N_{\text{aer}} = 300/\text{cc}$ (two-mode lognormal) $N_{\text{INP}} = 150/L$ (lognormal, $D_g = 0.74 \mu\text{m}$, $\sigma_g = 2.55$)

spin-up = freezing off; subsequently frozen particles act as tracers

particle-based μ -physics + prescribed-flow test

Time: 690 s (spin-up till 600.0 s)



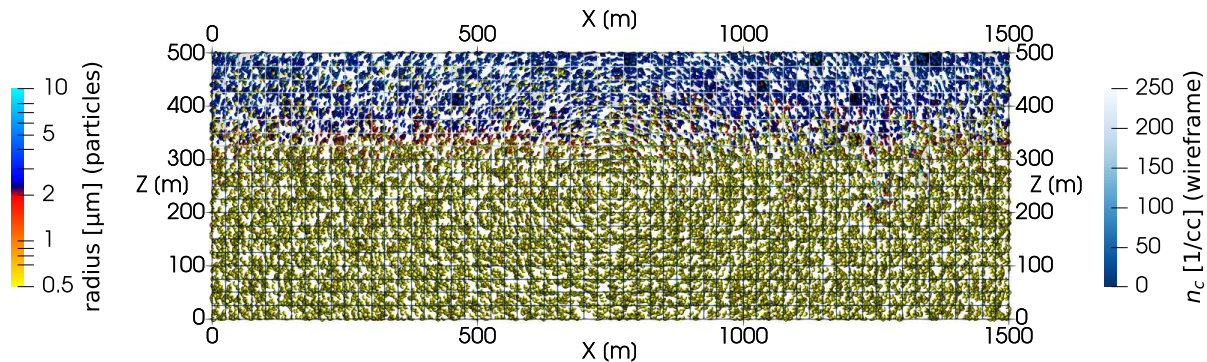
16+16 super-particles/cell for INP-rich + INP-free particles

$N_{\text{aer}} = 300/\text{cc}$ (two-mode lognormal) $N_{\text{INP}} = 150/L$ (lognormal, $D_g = 0.74 \mu\text{m}$, $\sigma_g = 2.55$)

spin-up = freezing off; subsequently frozen particles act as tracers

particle-based μ -physics + prescribed-flow test

Time: 720 s (spin-up till 600.0 s)



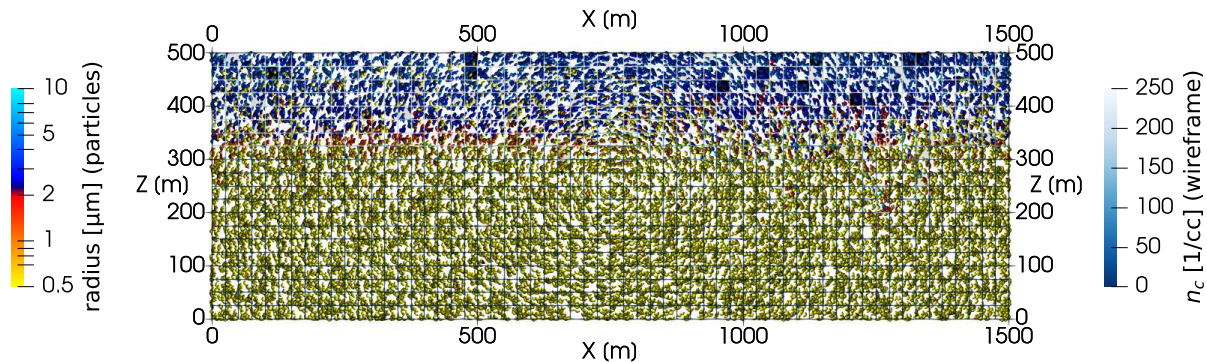
16+16 super-particles/cell for INP-rich + INP-free particles

$N_{\text{aer}} = 300/\text{cc}$ (two-mode lognormal) $N_{\text{INP}} = 150/L$ (lognormal, $D_g = 0.74 \mu\text{m}$, $\sigma_g = 2.55$)

spin-up = freezing off; subsequently frozen particles act as tracers

particle-based μ -physics + prescribed-flow test

Time: 750 s (spin-up till 600.0 s)



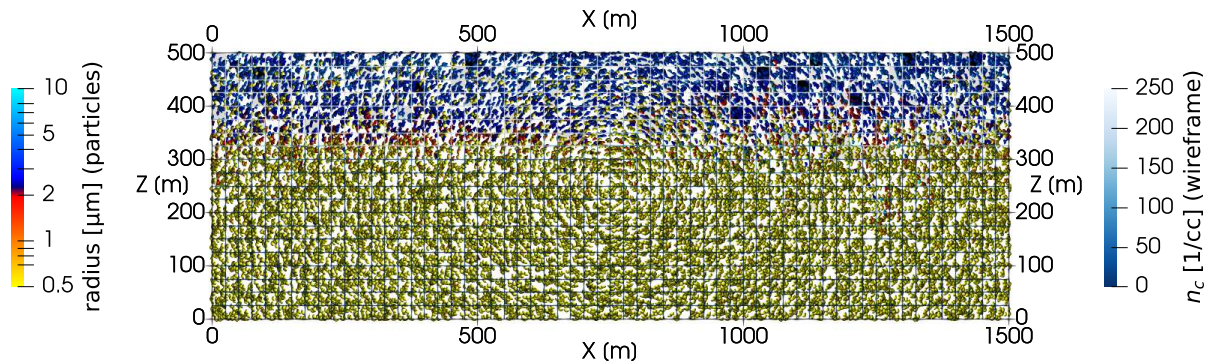
16+16 super-particles/cell for INP-rich + INP-free particles

$N_{\text{aer}} = 300/\text{cc}$ (two-mode lognormal) $N_{\text{INP}} = 150/L$ (lognormal, $D_g = 0.74 \mu\text{m}$, $\sigma_g = 2.55$)

spin-up = freezing off; subsequently frozen particles act as tracers

particle-based μ -physics + prescribed-flow test

Time: 780 s (spin-up till 600.0 s)



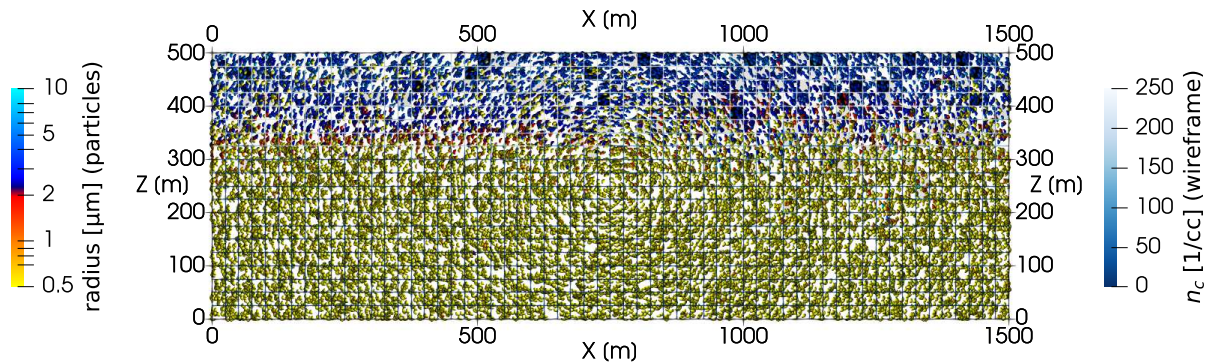
16+16 super-particles/cell for INP-rich + INP-free particles

$N_{\text{aer}} = 300/\text{cc}$ (two-mode lognormal) $N_{\text{INP}} = 150/L$ (lognormal, $D_g = 0.74 \mu\text{m}$, $\sigma_g = 2.55$)

spin-up = freezing off; subsequently frozen particles act as tracers

particle-based μ -physics + prescribed-flow test

Time: 810 s (spin-up till 600.0 s)



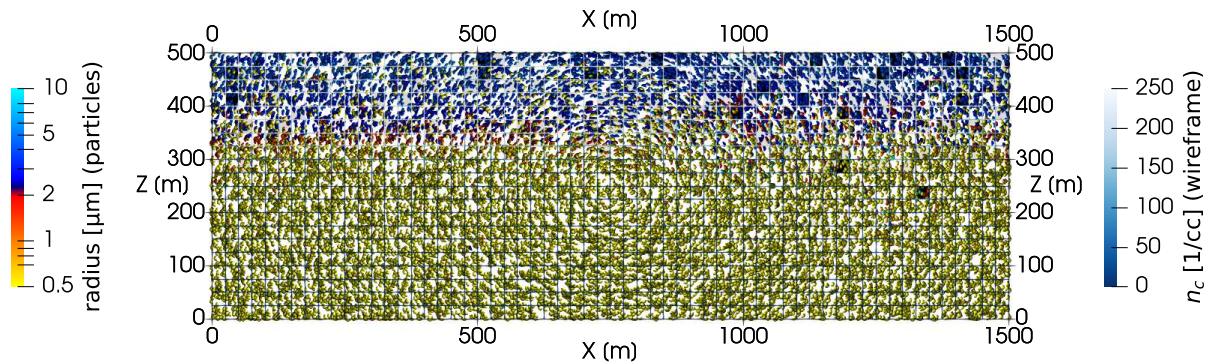
16+16 super-particles/cell for INP-rich + INP-free particles

$N_{\text{aer}} = 300/\text{cc}$ (two-mode lognormal) $N_{\text{INP}} = 150/L$ (lognormal, $D_g = 0.74 \mu\text{m}$, $\sigma_g = 2.55$)

spin-up = freezing off; subsequently frozen particles act as tracers

particle-based μ -physics + prescribed-flow test

Time: 840 s (spin-up till 600.0 s)



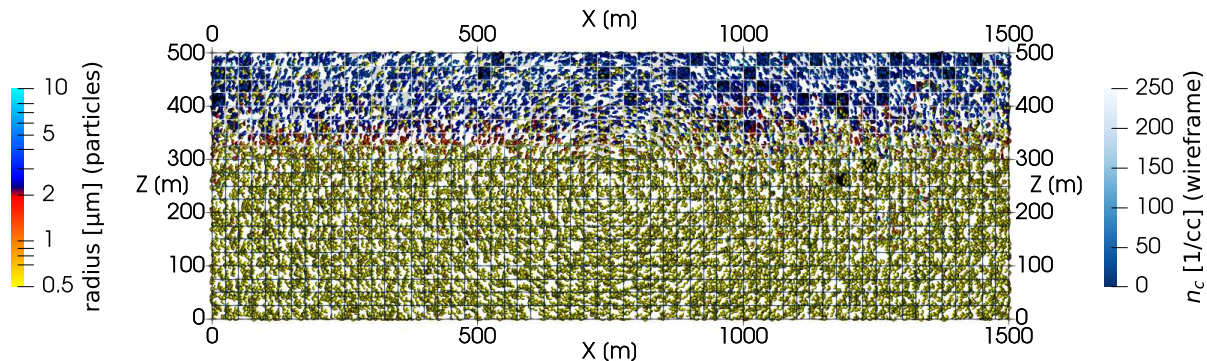
16+16 super-particles/cell for INP-rich + INP-free particles

$N_{\text{aer}} = 300/\text{cc}$ (two-mode lognormal) $N_{\text{INP}} = 150/L$ (lognormal, $D_g = 0.74 \mu\text{m}$, $\sigma_g = 2.55$)

spin-up = freezing off; subsequently frozen particles act as tracers

particle-based μ -physics + prescribed-flow test

Time: 870 s (spin-up till 600.0 s)



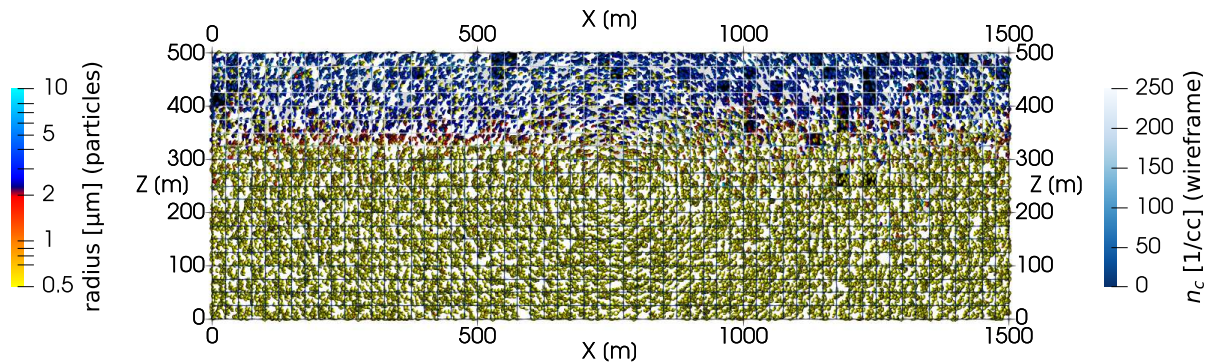
16+16 super-particles/cell for INP-rich + INP-free particles

$N_{\text{aer}} = 300/\text{cc}$ (two-mode lognormal) $N_{\text{INP}} = 150/L$ (lognormal, $D_g = 0.74 \mu\text{m}$, $\sigma_g = 2.55$)

spin-up = freezing off; subsequently frozen particles act as tracers

particle-based μ -physics + prescribed-flow test

Time: 900 s (spin-up till 600.0 s)



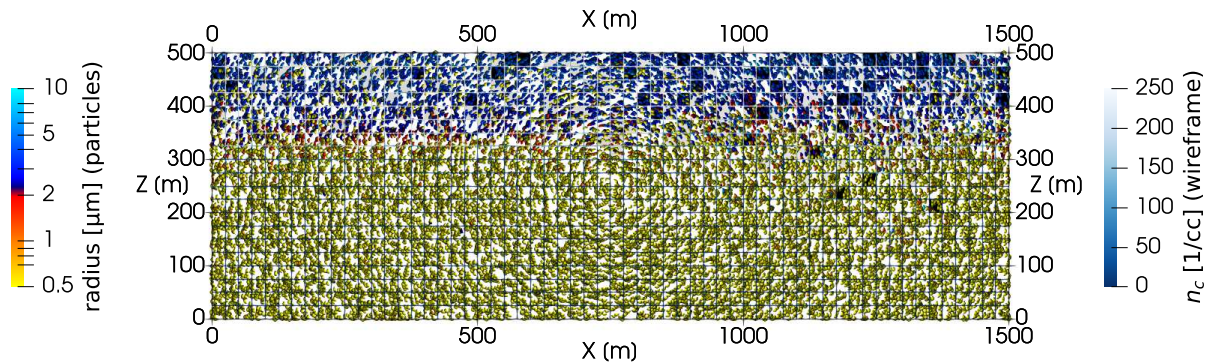
16+16 super-particles/cell for INP-rich + INP-free particles

$N_{\text{aer}} = 300/\text{cc}$ (two-mode lognormal) $N_{\text{INP}} = 150/L$ (lognormal, $D_g = 0.74 \mu\text{m}$, $\sigma_g = 2.55$)

spin-up = freezing off; subsequently frozen particles act as tracers

particle-based μ -physics + prescribed-flow test

Time: 930 s (spin-up till 600.0 s)



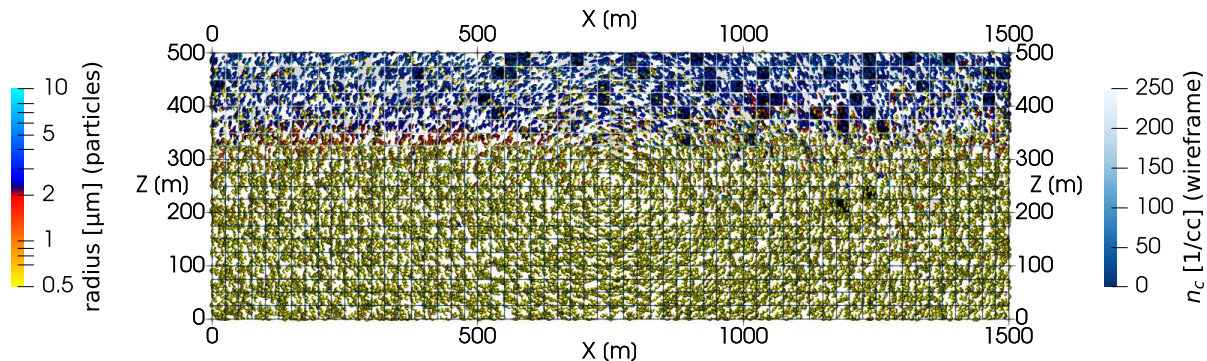
16+16 super-particles/cell for INP-rich + INP-free particles

$N_{\text{aer}} = 300/\text{cc}$ (two-mode lognormal) $N_{\text{INP}} = 150/L$ (lognormal, $D_g = 0.74 \mu\text{m}$, $\sigma_g = 2.55$)

spin-up = freezing off; subsequently frozen particles act as tracers

particle-based μ -physics + prescribed-flow test

Time: 960 s (spin-up till 600.0 s)



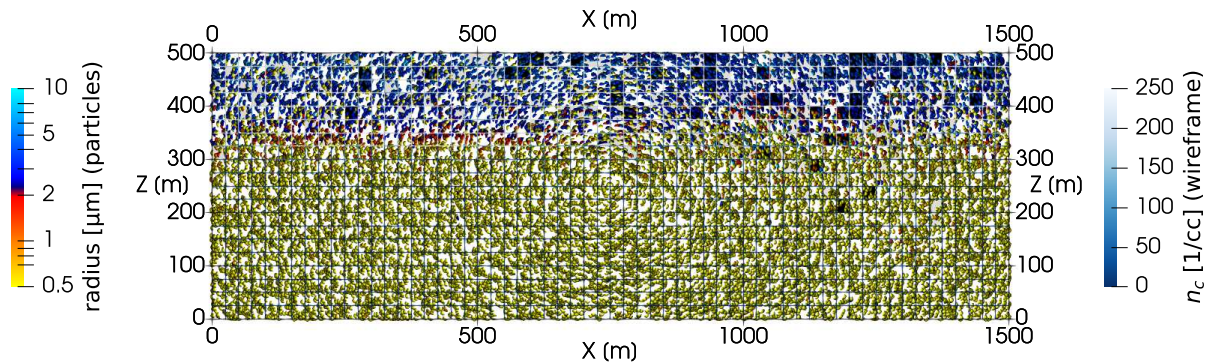
16+16 super-particles/cell for INP-rich + INP-free particles

$N_{\text{aer}} = 300/\text{cc}$ (two-mode lognormal) $N_{\text{INP}} = 150/L$ (lognormal, $D_g = 0.74 \mu\text{m}$, $\sigma_g = 2.55$)

spin-up = freezing off; subsequently frozen particles act as tracers

particle-based μ -physics + prescribed-flow test

Time: 990 s (spin-up till 600.0 s)



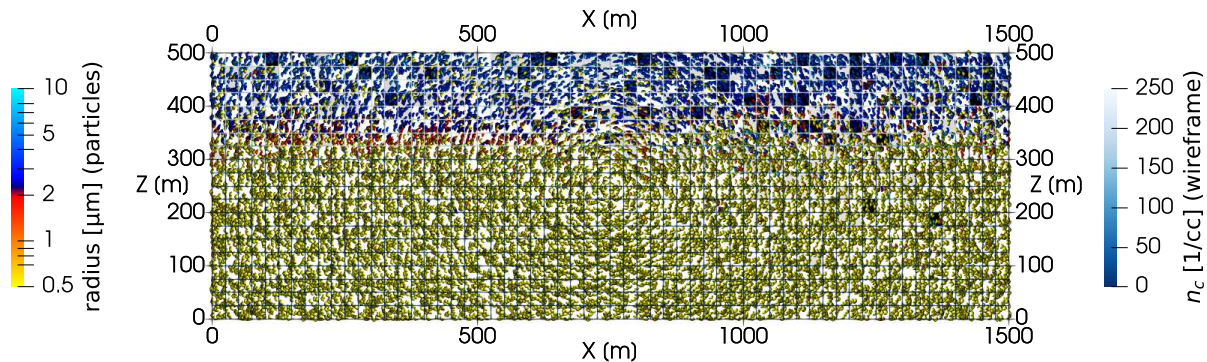
16+16 super-particles/cell for INP-rich + INP-free particles

$N_{\text{aer}} = 300/\text{cc}$ (two-mode lognormal) $N_{\text{INP}} = 150/L$ (lognormal, $D_g = 0.74 \mu\text{m}$, $\sigma_g = 2.55$)

spin-up = freezing off; subsequently frozen particles act as tracers

particle-based μ -physics + prescribed-flow test

Time: 1020 s (spin-up till 600.0 s)



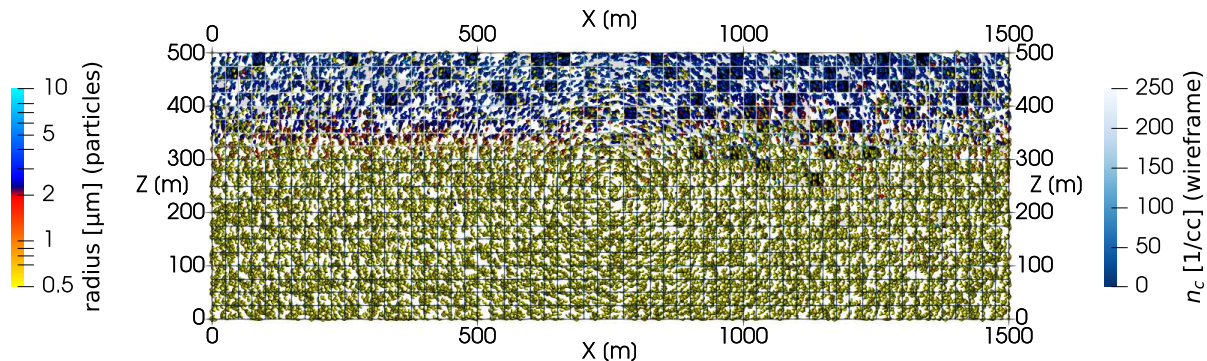
16+16 super-particles/cell for INP-rich + INP-free particles

$N_{\text{aer}} = 300/\text{cc}$ (two-mode lognormal) $N_{\text{INP}} = 150/L$ (lognormal, $D_g = 0.74 \mu\text{m}$, $\sigma_g = 2.55$)

spin-up = freezing off; subsequently frozen particles act as tracers

particle-based μ -physics + prescribed-flow test

Time: 1050 s (spin-up till 600.0 s)



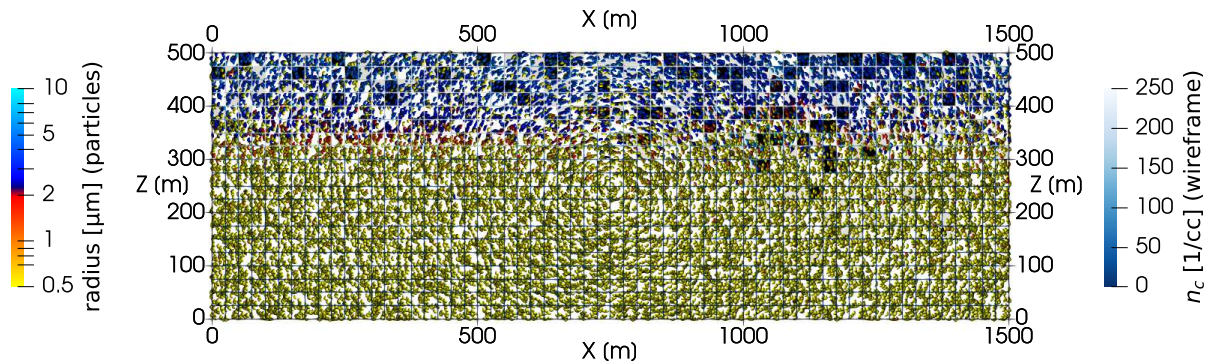
16+16 super-particles/cell for INP-rich + INP-free particles

$N_{\text{aer}} = 300/\text{cc}$ (two-mode lognormal) $N_{\text{INP}} = 150/L$ (lognormal, $D_g = 0.74 \mu\text{m}$, $\sigma_g = 2.55$)

spin-up = freezing off; subsequently frozen particles act as tracers

particle-based μ -physics + prescribed-flow test

Time: 1080 s (spin-up till 600.0 s)



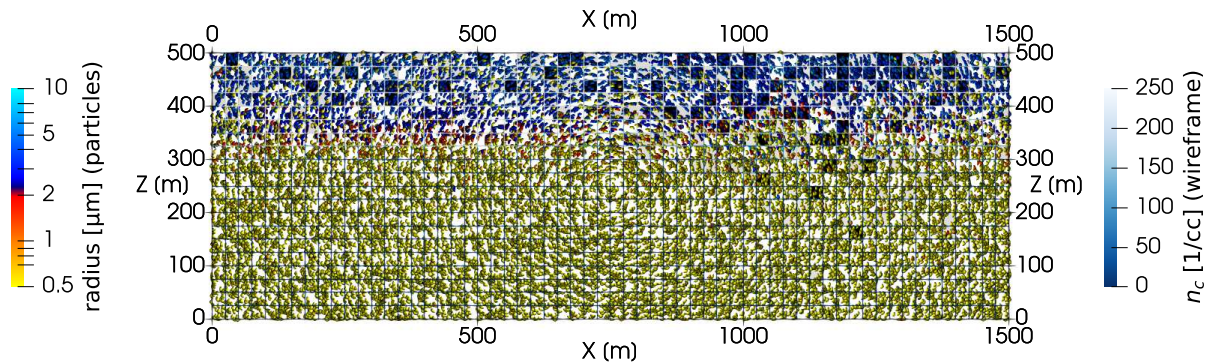
16+16 super-particles/cell for INP-rich + INP-free particles

$N_{\text{aer}} = 300/\text{cc}$ (two-mode lognormal) $N_{\text{INP}} = 150/L$ (lognormal, $D_g = 0.74 \mu\text{m}$, $\sigma_g = 2.55$)

spin-up = freezing off; subsequently frozen particles act as tracers

particle-based μ -physics + prescribed-flow test

Time: 1110 s (spin-up till 600.0 s)



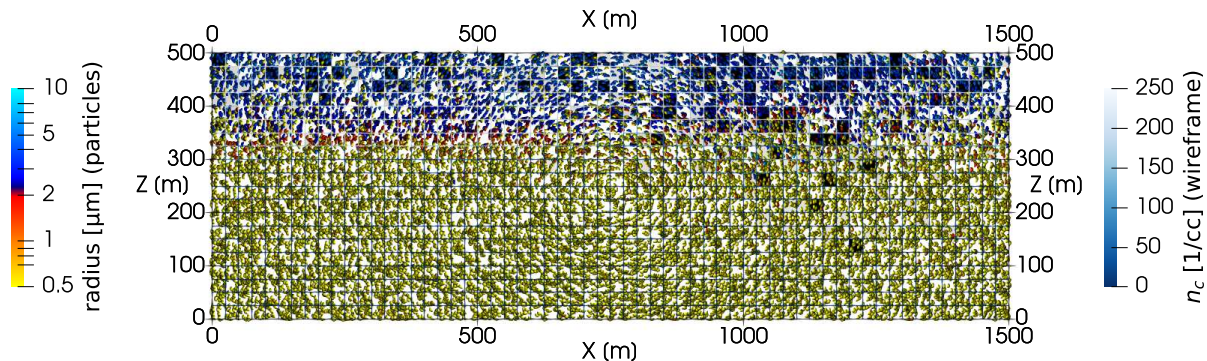
16+16 super-particles/cell for INP-rich + INP-free particles

$N_{\text{aer}} = 300/\text{cc}$ (two-mode lognormal) $N_{\text{INP}} = 150/L$ (lognormal, $D_g = 0.74 \mu\text{m}$, $\sigma_g = 2.55$)

spin-up = freezing off; subsequently frozen particles act as tracers

particle-based μ -physics + prescribed-flow test

Time: 1140 s (spin-up till 600.0 s)



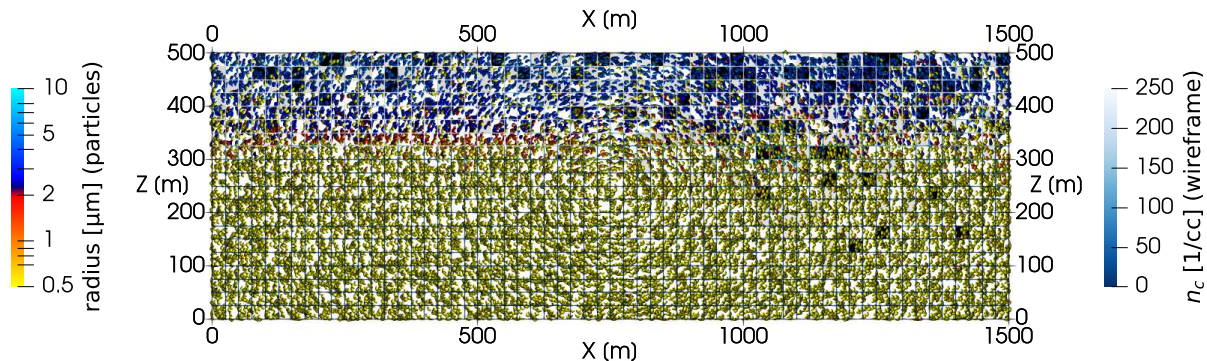
16+16 super-particles/cell for INP-rich + INP-free particles

$N_{\text{aer}} = 300/\text{cc}$ (two-mode lognormal) $N_{\text{INP}} = 150/L$ (lognormal, $D_g = 0.74 \mu\text{m}$, $\sigma_g = 2.55$)

spin-up = freezing off; subsequently frozen particles act as tracers

particle-based μ -physics + prescribed-flow test

Time: 1170 s (spin-up till 600.0 s)



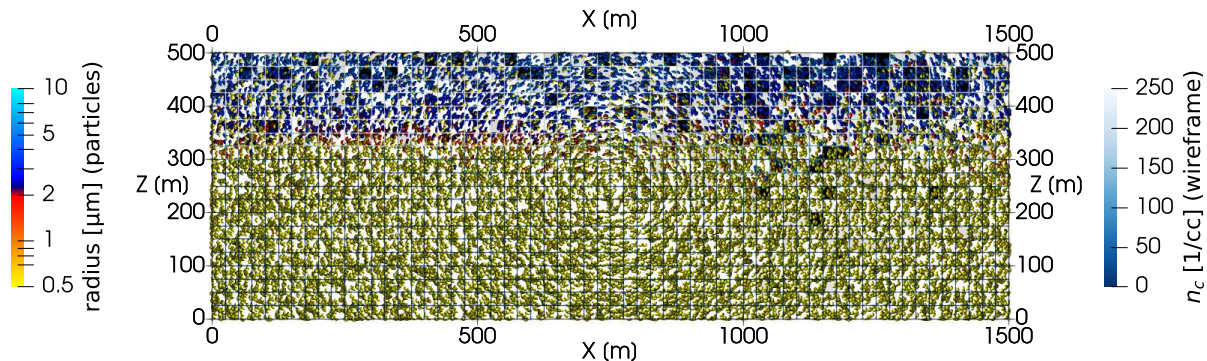
16+16 super-particles/cell for INP-rich + INP-free particles

$N_{\text{aer}} = 300/\text{cc}$ (two-mode lognormal) $N_{\text{INP}} = 150/L$ (lognormal, $D_g = 0.74 \mu\text{m}$, $\sigma_g = 2.55$)

spin-up = freezing off; subsequently frozen particles act as tracers

particle-based μ -physics + prescribed-flow test

Time: 1200 s (spin-up till 600.0 s)



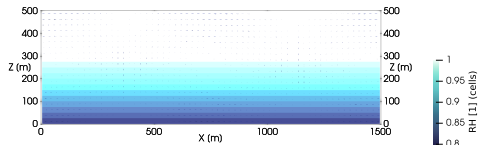
16+16 super-particles/cell for INP-rich + INP-free particles

$N_{\text{aer}} = 300/\text{cc}$ (two-mode lognormal) $N_{\text{INP}} = 150/L$ (lognormal, $D_g = 0.74 \mu\text{m}$, $\sigma_g = 2.55$)

spin-up = freezing off; subsequently frozen particles act as tracers

testing three flow regimes and two immersion freezing representations

$w_{\max} \approx 1/3 \text{ m/s}$

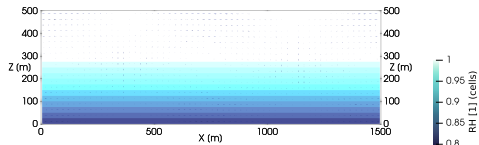


$w_{\max} \approx 1 \text{ m/s}$

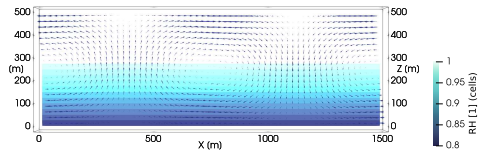
$w_{\max} \approx 3 \text{ m/s}$

testing three flow regimes and two immersion freezing representations

$w_{\max} \approx 1/3 \text{ m/s}$



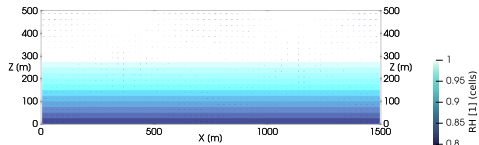
$w_{\max} \approx 1 \text{ m/s}$



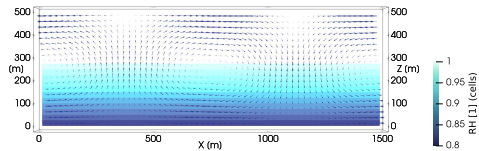
$w_{\max} \approx 3 \text{ m/s}$

testing three flow regimes and two immersion freezing representations

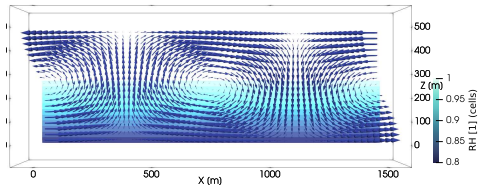
$W_{\max} \approx 1/3 \text{ m/s}$



$W_{\max} \approx 1 \text{ m/s}$

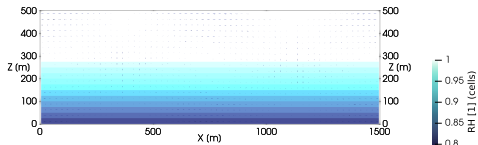


$W_{\max} \approx 3 \text{ m/s}$

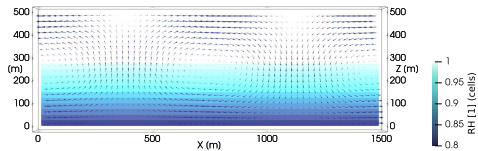


testing three flow regimes and two immersion freezing representations

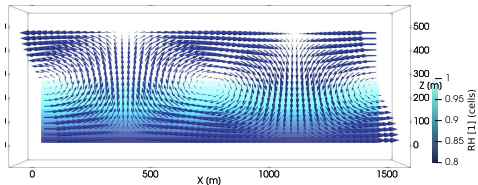
$w_{\max} \approx 1/3 \text{ m/s}$



$w_{\max} \approx 1 \text{ m/s}$

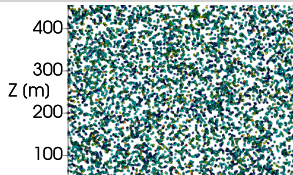


$w_{\max} \approx 3 \text{ m/s}$



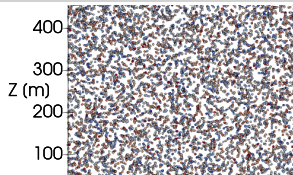
singular (INAS)

$T_{fz} \text{ [K (particles)]}$

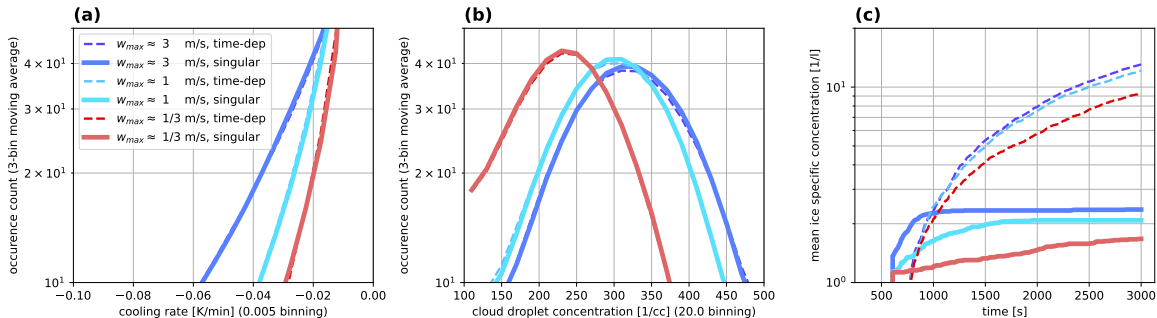


time-dependent (J_{het})

$A \text{ [}\mu\text{m}^2\text{]}$

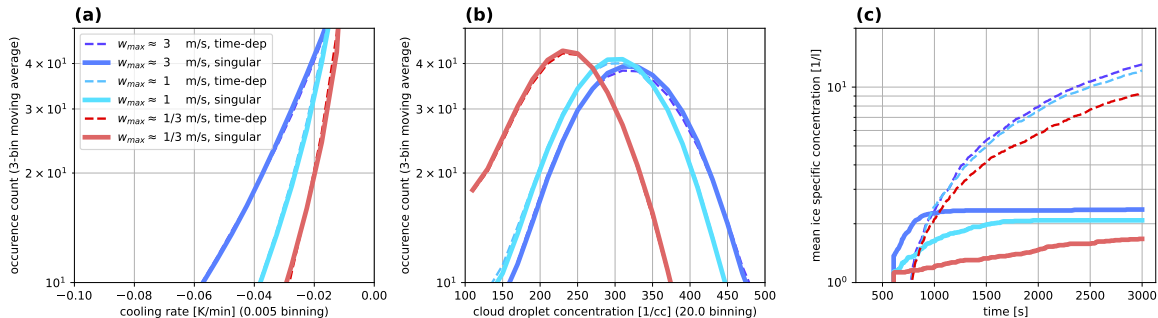


testing three flow regimes and two immersion freezing representations



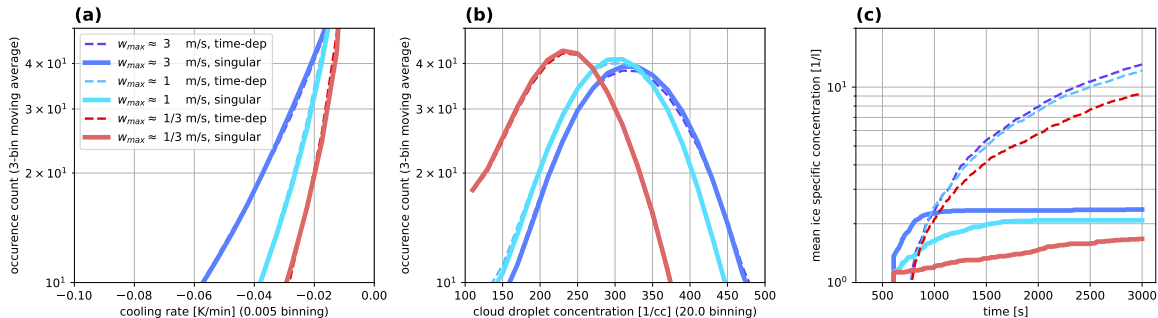
- ▶ range of cooling rates in simple flow (far from $c \sim 1$ K/min for AIDA as in Niemand et al. 2012)

testing three flow regimes and two immersion freezing representations

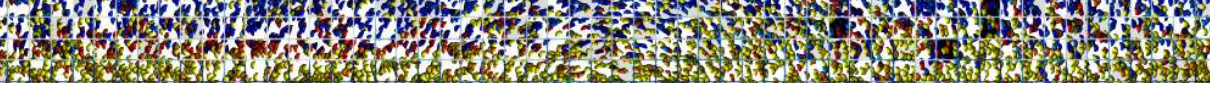


- ▶ range of cooling rates in simple flow (far from $c \sim 1$ K/min for AIDA as in Niemand et al. 2012)
- ▶ singular vs. time-dependent markedly different (consistent with box model for $c \ll 1$ K/min)

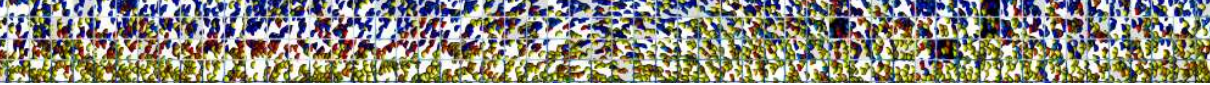
testing three flow regimes and two immersion freezing representations



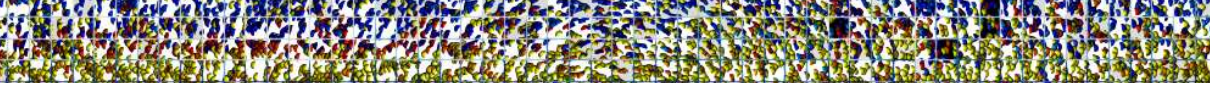
- ▶ range of cooling rates in simple flow (far from $c \sim 1$ K/min for AIDA as in Niemand et al. 2012)
- ▶ singular vs. time-dependent markedly different (consistent with box model for $c \ll 1$ K/min)
- ▶ CPU time trade off: time dependent ca. 3-4 times costlier



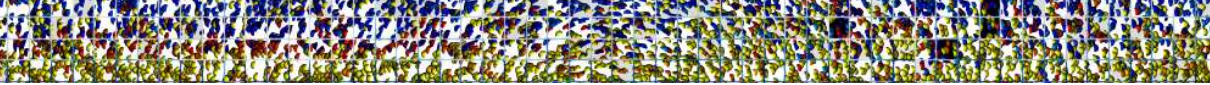
- ▶ this study: **ABIFM-based time-dependent particle-based immersion freezing**



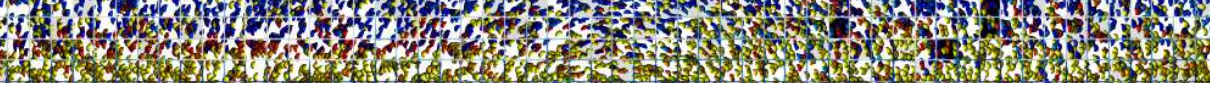
- ▶ this study: **ABIFM-based time-dependent particle-based immersion freezing**
 - ▶ box examples: role of INP size spectral width (same for time-dependent and singular)



- ▶ this study: **ABIFM-based time-dependent particle-based immersion freezing**
 - ▶ box examples: role of INP size spectral width (same for time-dependent and singular)
 - ▶ box & 2D: cooling rate embedded in INAS fits \rightsquigarrow limited robustness to different flow regimes



- ▶ this study: **ABIFM-based time-dependent particle-based immersion freezing**
 - ▶ box examples: role of INP size spectral width (same for time-dependent and singular)
 - ▶ box & 2D: cooling rate embedded in INAS fits \rightsquigarrow limited robustness to different flow regimes
 - ▶ both particle-based schemes (singular and time-dependent) resolve INP reservoir



- ▶ **this study: ABIFM-based time-dependent particle-based immersion freezing**
 - ▶ box examples: role of INP size spectral width (same for time-dependent and singular)
 - ▶ box & 2D: cooling rate embedded in INAS fits \rightsquigarrow limited robustness to different flow regimes
 - ▶ both particle-based schemes (singular and time-dependent) resolve INP reservoir
 - ▶ implementation in PySDM (both singular and time-dependent)



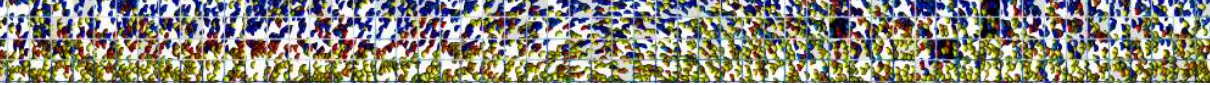
- ▶ this study: **ABIFM-based time-dependent particle-based immersion freezing**
 - ▶ box examples: role of INP size spectral width (same for time-dependent and singular)
 - ▶ box & 2D: cooling rate embedded in INAS fits \rightsquigarrow limited robustness to different flow regimes
 - ▶ both particle-based schemes (singular and time-dependent) resolve INP reservoir
 - ▶ implementation in PySDM (both singular and time-dependent)

- ▶ next steps:



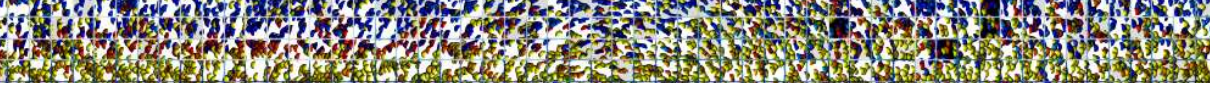
- ▶ this study: **ABIFM-based time-dependent particle-based immersion freezing**
 - ▶ box examples: role of INP size spectral width (same for time-dependent and singular)
 - ▶ box & 2D: cooling rate embedded in INAS fits \rightsquigarrow limited robustness to different flow regimes
 - ▶ both particle-based schemes (singular and time-dependent) resolve INP reservoir
 - ▶ implementation in PySDM (both singular and time-dependent)

- ▶ next steps:
 - ▶ leverage particle-resolved representation to simulate diverse INP populations



- ▶ this study: **ABIFM-based time-dependent particle-based immersion freezing**
 - ▶ box examples: role of INP size spectral width (same for time-dependent and singular)
 - ▶ box & 2D: cooling rate embedded in INAS fits \rightsquigarrow limited robustness to different flow regimes
 - ▶ both particle-based schemes (singular and time-dependent) resolve INP reservoir
 - ▶ implementation in PySDM (both singular and time-dependent)

- ▶ next steps:
 - ▶ leverage particle-resolved representation to simulate diverse INP populations
 - ▶ inform larger-scale models with results from detailed particle-resolved simulations



- ▶ this study: **ABIFM-based time-dependent particle-based immersion freezing**
 - ▶ box examples: role of INP size spectral width (same for time-dependent and singular)
 - ▶ box & 2D: cooling rate embedded in INAS fits \rightsquigarrow limited robustness to different flow regimes
 - ▶ both particle-based schemes (singular and time-dependent) resolve INP reservoir
 - ▶ implementation in PySDM (both singular and time-dependent)
- ▶ next steps:
 - ▶ leverage particle-resolved representation to simulate diverse INP populations
 - ▶ inform larger-scale models with results from detailed particle-resolved simulations

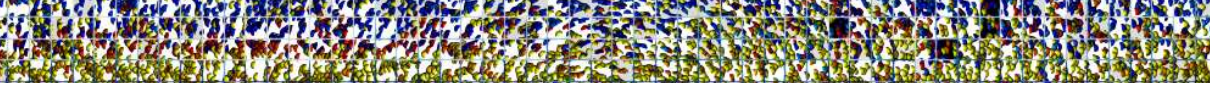


ASR

Atmospheric
System Research

DOE ASR grant no.

DE-SC0021034



- ▶ this study: **ABIFM-based time-dependent particle-based immersion freezing**
 - ▶ box examples: role of INP size spectral width (same for time-dependent and singular)
 - ▶ box & 2D: cooling rate embedded in INAS fits \rightsquigarrow limited robustness to different flow regimes
 - ▶ both particle-based schemes (singular and time-dependent) resolve INP reservoir
 - ▶ implementation in PySDM (both singular and time-dependent)
- ▶ next steps:
 - ▶ leverage particle-resolved representation to simulate diverse INP populations
 - ▶ inform larger-scale models with results from detailed particle-resolved simulations



ASR

Atmospheric
System Research

DOE ASR grant no.

DE-SC0021034

project hosted at:

I ILLINOIS

- 
- ▶ this study: **ABIFM-based time-dependent particle-based immersion freezing**
 - ▶ box examples: role of INP size spectral width (same for time-dependent and singular)
 - ▶ box & 2D: cooling rate embedded in INAS fits \rightsquigarrow limited robustness to different flow regimes
 - ▶ both particle-based schemes (singular and time-dependent) resolve INP reservoir
 - ▶ implementation in PySDM (both singular and time-dependent)
 - ▶ next steps:
 - ▶ leverage particle-resolved representation to simulate diverse INP populations
 - ▶ inform larger-scale models with results from detailed particle-resolved simulations



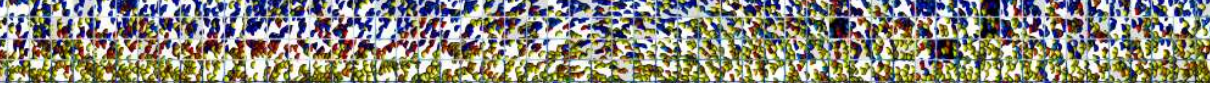
DOE ASR grant no.
DE-SC0021034

project hosted at:

I ILLINOIS

open  python™ code:

 /atmos-cloud-sim-uj



- ▶ this study: **ABIFM-based time-dependent particle-based immersion freezing**
 - ▶ box examples: role of INP size spectral width (same for time-dependent and singular)
 - ▶ box & 2D: cooling rate embedded in INAS fits \rightsquigarrow limited robustness to different flow regimes
 - ▶ both particle-based schemes (singular and time-dependent) resolve INP reservoir
 - ▶ implementation in PySDM (both singular and time-dependent)
- ▶ next steps:
 - ▶ leverage particle-resolved representation to simulate diverse INP populations
 - ▶ inform larger-scale models with results from detailed particle-resolved simulations



DOE ASR grant no.
DE-SC0021034

project hosted at:

I ILLINOIS

open  python™ code:

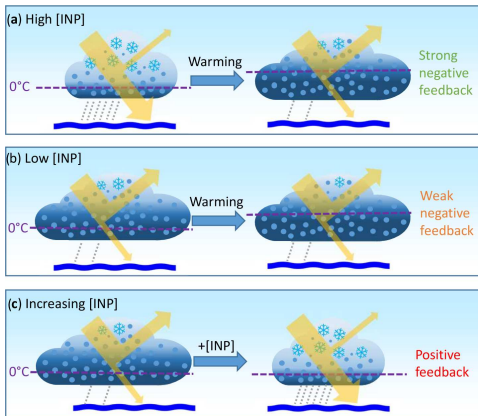
 /atmos-cloud-sim-uj



Thank you
for the invitation!

Opinion: Cloud-phase climate feedback and the importance of ice-nucleating particles

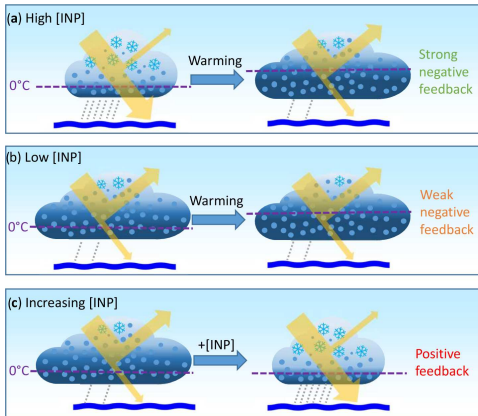
Benjamin J. Murray¹, Kenneth S. Carslaw¹, and Paul R. Field^{1,2}



- *"it is becoming very clear that the cloud-phase feedback contributes substantially to the uncertainty in predictions of the rate at which our planet will warm in response to CO₂ emissions"*

Opinion: Cloud-phase climate feedback and the importance of ice-nucleating particles

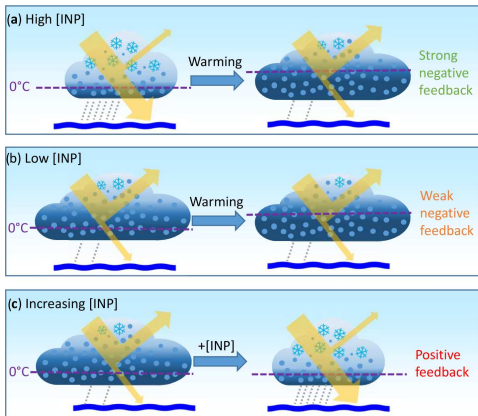
Benjamin J. Murray¹, Kenneth S. Carslaw¹, and Paul R. Field^{1,2}



- ▶ *"it is becoming very clear that the cloud-phase feedback contributes substantially to the uncertainty in predictions of the rate at which our planet will warm in response to CO₂ emissions"*
- ▶ *"core physical process that drives the cloud-phase feedback is the transition to clouds with more liquid water and less ice as the isotherms shift upwards in a warmer world"*

Opinion: Cloud-phase climate feedback and the importance of ice-nucleating particles

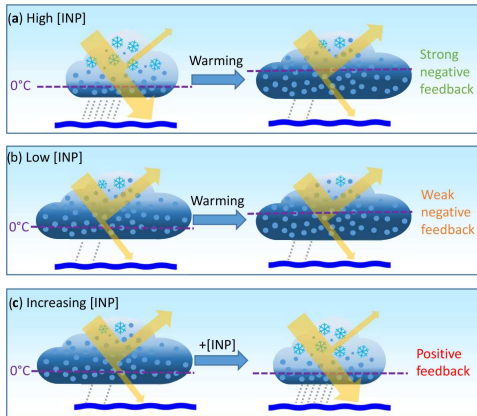
Benjamin J. Murray¹, Kenneth S. Carslaw¹, and Paul R. Field^{1,2}



- ▶ *"it is becoming very clear that the cloud-phase feedback contributes substantially to the uncertainty in predictions of the rate at which our planet will warm in response to CO₂ emissions"*
- ▶ *"core physical process that drives the cloud-phase feedback is the transition to clouds with more liquid water and less ice as the isotherms shift upwards in a warmer world"*
- ▶ *"models need to improve their representation of ice-related microphysical processes; in particular, they need to include a direct link to aerosol type, specifically INPs"*

Opinion: Cloud-phase climate feedback and the importance of ice-nucleating particles

Benjamin J. Murray¹, Kenneth S. Carslaw¹, and Paul R. Field^{1,2}



- ▶ *"it is becoming very clear that the cloud-phase feedback contributes substantially to the uncertainty in predictions of the rate at which our planet will warm in response to CO₂ emissions"*
- ▶ *"core physical process that drives the cloud-phase feedback is the transition to clouds with more liquid water and less ice as the isotherms shift upwards in a warmer world"*
- ▶ *"models need to improve their representation of ice-related microphysical processes; in particular, they need to include a direct link to aerosol type, specifically INPs"*
- ▶ *"must also represent the INP removal processes, which in turn depend on a correct representation of the microphysics"*